Automatica 132 (2021) 109807

Contents lists available at ScienceDirect

Automatica

journal homepage: www.elsevier.com/locate/automatica

Scalable resetting algorithms for synchronization of pulse-coupled oscillators over rooted directed graphs☆

Muhammad Umar Javed *, Jorge I. Poveda, Xudong Chen

Department of Electrical, Computer, and Energy Engineering, University of Colorado Boulder, Boulder, CO 80309, United States of America

ARTICLE INFO

Article history:
Received 16 May 2020
Received in revised form 26 February 2021
Accepted 31 May 2021
Available online 24 July 2021

Keywords:
Networked systems
Synchronization of multi-agent systems
Hybrid dynamical systems
Stochastic processes

ABSTRACT

We study the problem of robust global synchronization of pulse-coupled oscillators (PCOs) over directed graphs. It is known that when the digraphs are strongly connected, global synchronization can be achieved by using a class of deterministic binary set-valued resetting controllers (Poveda and Teel, 2019). However, for large-scale networks, these algorithms are not scalable because some of their tuning parameters have upper bounds of the order $\mathcal{O}\left(\frac{1}{N}\right)$, where N is the number of agents. This paper resolves this scalability issue by presenting several new results about global synchronization of PCOs with more general network topologies using the frameworks of deterministic and stochastic hybrid dynamical systems. First, we establish that similar deterministic binary resetting algorithms can achieve robust global and fixed-time synchronization in any *rooted acyclic digraph*. Moreover, in this case, we show that the synchronization dynamics are now scalable as the tuning parameters of the algorithm are *network independent*, i.e., of order $\mathcal{O}(1)$. However, the algorithms cannot be further extended to all rooted digraphs. We establish this new impossibility result by introducing a counter-example with a particular rooted digraph for which global synchronization cannot be achieved, irrespective of the tuning parameters. Nevertheless, we show that if the binary resetting algorithms are modified by accommodating an Erdös–Renýi type random graph model, then the resulting stochastic resetting dynamics will guarantee global synchronization almost surely for all *rooted digraphs* and, moreover, the tuning parameters of the dynamics are network independent. Stability and robustness properties of the resetting algorithms are studied using the tools from set-valued hybrid dynamical systems. Numerical simulations are provided at the end of the paper for demonstration of the main results.

1. Introduction

A network of pulse-coupled oscillators (PCOs) consists of N periodic dynamical systems, also called agents, sharing information via a communication directed graph (digraph). In most of the standard models of PCOs, e.g., Kannapan and Bullo (2016), Nunez, Wang, and Doyle (2015a), Pagliari and Scaglione (2011), Poveda and Teel (2019a) and Proskurnikov and Cao (2017), each agent has an individual state $\tau_i \in \mathbb{R}$, which evolves according to the following continuous-time dynamics:

$$\tau_i \in [0, 1) \implies \dot{\tau}_i = \frac{1}{T}, \quad \forall\, i \in \{1, 2, \ldots, N\}, \tag{1}$$

where $T > 0$ is the period of the oscillator, and $[0, 1)$ is a normalized unit interval. When the state of an agent i finishes an oscillation, it sends a pulse to its out-neighbors j (the information flow topology will be described by a directed graph, and j is an out-neighbor of i if (i, j) is an edge of the graph), and it proceeds to instantaneously *reset* its individual state back to zero:

$$\tau_i = 1 \implies \tau_i^+ = 0. \tag{2}$$

After receiving the pulse, each out-neighbor j of agent i instantaneously updates its own state τ_j using an individual phase update rule (PR) $\tau_j \mapsto \mathcal{P}_j(\tau_j)$, which usually has the following form:

$$\tau_j^+ = \mathcal{P}_j(\tau_j) = \begin{cases} B(\tau_j), & \text{if } \tau_j \in [0, r_j), \\ F(\tau_j), & \text{if } \tau_j \in [r_j, 1). \end{cases} \tag{3}$$

The mapping $\tau_j \mapsto B_j(\tau_j)$ is commonly referred to as the *backward mapping*, and it decreases the value of τ_j. The mapping

☆ The work is supported by National Science Foundation, United States of America under Grants ECCS-1809315 and CRII: CNS-1947613, and AFOSR, United States of America under Grant FA9550-20-1-0076. The material in this paper was partially presented at the 58th IEEE Conference on Decision and Control, December 11–13, 2019, Nice, France. This paper was recommended for publication in revised form by Associate Editor Florian Dorfler under the direction of Editor Christos G. Cassandras.

* Corresponding author.
E-mail addresses: muhammad.javed@colorado.edu (M.U. Javed), jorge.poveda@colorado.edu (J.I. Poveda), xudong.chen@colorado.edu (X. Chen).

https://doi.org/10.1016/j.automatica.2021.109807
0005-1098/

$\tau_j \mapsto F_j(\tau_j)$ is referred to as the *forward mapping*, and it increases τ_j (Kannapan & Bullo, 2016). Whether an agent j implements the mapping B_j or the mapping F_j, depends on the position of τ_j with respect to the constant $r_j \in [0, 1)$, which partitions in Eq. (3) the normalized unit interval of each agent. In this way, PCOs can be seen as multi-agent dynamical systems that combine the continuous-time dynamics (1) and the discrete-time dynamics (2)–(3). As a consequence, they are naturally modeled as networked multi-agent hybrid dynamical systems (Poveda & Teel, 2019b), and their convergence and stability properties are highly dependent on the structures of the mappings $\mathcal{P}_j$ and the partitions induced by the tuning parameters r_j.

Given that Eqs. (1)–(3) are quite general, PCOs can be used to model different biological systems, including Cardiac pacemakers, rhythmic flashing of fireflies, electrical signals of neurons, and biological oscillators, see Kannapan and Bullo (2016) and references therein. Networks of PCOs have also found several applications in engineering systems, such as cellular mobile radio (Tyrrell, 2009), sensor networks (Wang & Doyle, 2012; Wang, Nunez, & Doyle, 2012, 2013), and autonomous vehicles (Sepulchre, Paley, & Leonard, 2007). Owing to the property of fixed time convergence, PCOs with *binary* phase update rules have attracted more and more attentions and have been used to address a variety of engineering problems. Specifically, they have been used to synchronize and coordinate clocks and logic states in networks of sampled-data systems (Poveda & Teel, 2019a; Teel & Poveda, 2015), and also in distributed optimization algorithms with local timers (Ochoa, Poveda, Uribe, & Quijano, 2021). In these applications, it is of interest to achieve fixed-time exact synchronization to emulate a centralized system having one single timer that coordinates the network. Finally, we refer the reader to Section 1.2 of the survey paper (Dörfler & Bullo, 2014) for more relevant applications of PCOs.

A particular feature of PCOs is that their individual states are confined to evolve in the normalized interval [0, 1]. By embedding the closed interval to the unit circle and identifying the two points 0 and 1 with each other, the network of PCOs can be viewed as a multi-agent system evolving on the N-torus, where the state τ_i of the ith agent evolves in the unit circle flowing in counter-clockwise direction with frequency $1/T$. In this way, achieving global synchronization of PCOs can be cast as a global stabilization problem on a smooth compact manifold (Poveda & Teel, 2019a; Sontag, 1999a). It is well-known that there is no smooth continuous-time state-feedback control law that can solve, in a robust way, such type of stabilization problems (Dörfler & Bullo, 2014; Sontag, 1999a, 1999b). This impossibility result has motivated the development of several synchronization algorithms that relax the global convergence requirement and, instead, focus on achieving only *local* convergence (Kannapan & Bullo, 2016; Kuramoto, 1991; Nishimura & Friedman, 2011; Phillips, Sanfelice, & Erwin, 2012; Wang & Wang, 2020a) or *almost global* synchronization results, i.e., synchronization from all initial conditions except possibly from those in a set of measure zero (Mauroy & Sepulchre, 2012; Nishimura & Friedman, 2012; Proskurnikov & Cao, 2017; Sarlette & Sepulchre, 2009). However, for applications where measurement noise or external disturbances are unavoidable, almost global convergence results can be problematic given that they lead to non-zero measure sets from which synchronization cannot be achieved under arbitrarily small disturbances (Mayhew, 2010; Sontag, 1999b). Moreover, such problematic non-zero measure sets can be quite large in multi-agent systems when the number of agents is large.

On the other hand, it has been shown that *global* synchronization of PCOs can be achieved by using a hybrid-system approach over various network topologies, such as cycle digraphs (Nunez et al., 2015a), strongly rooted digraphs (Nunez, Wang, Teel, & Doyle, 2016), bidirectional chains and directed trees in Gao and Wang (2019), bidirectional digraphs (Nunez, Wang, & Doyle, 2015b), and complete digraphs (Canavier & Tikidji-Hamburyan, 2017). Relevant issues, such as resilience of global synchronization under attacks, have also been investigated in the literature (Wang & Wang, 2018, 2020b). In terms of convergence time (i.e., time for PCOs to reach synchronization), we refer the reader to Canavier and Tikidji-Hamburyan (2017), Gao and Wang (2019), Nunez et al. (2015a, 2015b, 2016) and Wang and Wang (2018) for asymptotic convergence and to Poveda and Teel (2019a), Teel and Poveda (2015) and Wang and Wang (2020b) for fixed-time convergence.

Using hybrid dynamics, robustness of synchronization can be established by considering well-posed set-valued regularizations of the discontinuous PR (3); see Gao and Wang (2019). The set-valued hybrid model has also been investigated in Poveda and Teel (2019a) and Teel and Poveda (2015) using (deterministic) binary phase update rules (BPRs) that satisfy $\mathcal{P}_j : [0, 1] \rightrightarrows \{0, 1\}$, i.e., mappings that reset the position of each agent to a given point in the unit circle that identifies the beginning and the end of the interval [0, 1]. By using this type of resetting rule, also called *strong firing* (Nishimura, 2013), it was shown in Poveda and Teel (2019a) and Teel and Poveda (2015) that global and robust *fixed-time* synchronization of homogeneous PCOs can be achieved if the underlying information flow topology is characterized by a directed *strongly connected* graph and if all the tuning parameters r_j satisfy an upper bound of order $\mathcal{O}\left(\frac{1}{N}\right)$, see, e.g., Poveda and Teel (2019a, Thm. 1). Thus, as the size of the network increases, the set of feasible parameters goes to zero, resulting in a scalability issue that holds even for strongly connected digraphs. Besides the scalability issue, it has also remained an open question what type of directed graphs, other than the strongly connected ones, are necessary and/or sufficient for synchronization in PCOs with binary resetting rules.

In this paper we address both questions at a time. We characterize a class of digraphs, namely graphs that are rooted acyclic, for which *robust*, *global*, and *fixed-time* synchronization can be achieved by using resetting algorithms with BPRs. In this case, the algorithms are scalable because the tuning parameters r_j are independent of network size. This result further allows us to extend the resetting algorithm to a stochastic setting, where a sequence of independent, identically distributed (*i.i.d.*) Bernoulli random variables is used by each agent i to decide whether or not to send the impulses to the out-neighbors j after resetting its own state via equation (2). Interestingly, by injecting this randomness into the networked system, synchronization can be achieved almost surely for the entire class of rooted digraphs. Moreover, we show that with such digraphs it is in general impossible to achieve global synchronization using the deterministic resetting algorithm. We outline below the main contributions of the paper:

(1) We show in Proposition 2 that having a rooted digraph is *necessary* for achieving global synchronization of PCOs using deterministic BPRs. However, as shown in Proposition 3, this condition is not sufficient, which is true regardless of the choices of tuning parameters of the BPRs. Note that the gap between necessity and sufficiency makes our problem different from standard consensus dynamics in Euclidean spaces where having a rooted digraph is generally sufficient for global synchronization.

(2) We show that if the underlying digraph is rooted acyclic, then the deterministic resetting algorithm achieves global and fixed-time synchronization. Moreover, the tuning parameters of individual PCOs are network independent. The result is formulated as Theorem 1, and extended in Corollary 1 to quasi-acyclic digraphs. In each case, we provide a clear characterization of the upper bounds of the convergence time in terms of the depth of the digraph.

(3) We show that in the stochastic setting (with random triggers of pulses), the corresponding resetting algorithm can achieve global synchronization almost surely for *all* rooted digraphs. Moreover, we show that the probability of the network reaching synchronization converges exponentially fast to one. The tuning parameters are again independent of the network size. The result is in contrast with the counter-example provided in Proposition 3 for the deterministic setting.

By the nature of the dynamics of the PCOs, we combine graph theoretic tools (Bullo, 2019) and set-valued hybrid dynamical system's (HDS) theory (Goebel, Sanfelice, & Teel, 2012) to analyze the qualitative properties of the network. This formalism is instrumental to the robustness analysis of the synchronization dynamics with respect to small additive bounded disturbances that are unavoidable in practice. To the best of author's knowledge, the results of this paper are the first ones that address the *scalability* issue that emerges in the global synchronization problem of PCOs, and that establish *robust global* synchronization over quasi-acyclic digraphs without using leading agents or global cues, with an explicit characterization of the convergence time as a function of the structure of the digraph. Moreover, unlike existing almost sure convergence results in the literature of stochastic synchronization of PCOs, e.g., Hartman, Subbaraman, and Teel (2013), Klinglmayr, Bettstetter, Timme, and Kirst (2017), Klinglmayr, Kirst, Bettstetter, and Timme (2012) and Pagliari and Scaglione (2011), we use the framework of stochastic hybrid dynamical systems to establish uniform global asymptotic stability in probability of the PCOs, with respect to the synchronization set, in rooted digraphs. Furthermore, we provide theoretical bounds for the stochastic synchronization time of our algorithms, as functions of the structures of the underlying digraphs. Our results open the door to new potential applications in the context of distributed control and optimization in networked systems with local timers that require synchronization mechanisms over general rooted digraphs (Ochoa et al., 2021; Poveda & Teel, 2019a; Teel & Poveda, 2015). Earlier, preliminary results, reported in the conference paper (Javed, Poveda, & Chen, 2019), considered only deterministic algorithms and presented results only for rooted acyclic digraphs, a subclass of the digraphs considered in this paper. Analysis and proofs of the results were also omitted in the conference version.

The rest of this paper is organized as follows: Section 2 presents some preliminaries. Main results for the deterministic and stochastic settings are presented and established in Sections 3 and 4 , respectively. Section 5 shows numerical examples. The paper ends with conclusions.

Notations. Given a vector $x \in \mathbb{R}^n$, we let $|x|$ be the Euclidean norm of x. For a compact set $\mathcal{A} \subset \mathbb{R}^n$, we let $|x|_{\mathcal{A}} := \min_{y\in\mathcal{A}} |x-y|$. We also use $|\cdot|$ to denote the cardinality of a set. We use $c_n \in \mathbb{R}^n$ to denote a constant vector with all entries equal to $c \in \mathbb{R}$. We use $\mathbb{S} \subset \mathbb{R}^2$ to denote the unit circle centered at the origin, i.e., $\mathbb{S} := \{(x_1, x_2) \in \mathbb{R}^2 : x_1^2 + x_2^2 = 1\}$. Given a set B, we use B^N to denote the N-Cartesian product of B, i.e., $B^N := B \times B \times \cdots \times B$. A function β is said to be of class $\mathcal{KL}$ if it is non-decreasing in its first argument, non-increasing in its second argument, $\lim_{r\to 0^+} \beta(r,s) = 0$ for each $s \in \mathbb{R}_{\geq 0}$, and $\lim_{s\to\infty} \beta(r,s) = 0$ for each $r \in \mathbb{R}_{\geq 0}$. For a closed set $B \subset \mathbb{R}^n$, and $\varepsilon > 0$, $B + \varepsilon\mathbb{B}$ denotes the set $\{x \in \mathbb{R}^n : |x|_B \leq \varepsilon\}$. We use $\mathbb{B}^\circ$ to denote an open ball of radius one centered at zero. For a real number x, we denote by $\lfloor x \rfloor$ the maximum integer that is less than or equal to x.

2. Preliminaries

This section presents basic notions from graph theory, hybrid dynamical systems, and notions of system stability.

2.1. Basic notions from graph theory

A directed graph, or digraph, is denoted by $\mathcal{G} := (\mathcal{V}, \mathcal{E})$, and it is characterized by the set of vertices $\mathcal{V} := \{1, 2, \ldots, N\}$, and the set of edges $\mathcal{E} \subset \mathcal{V} \times \mathcal{V}$. In this paper, we consider only simple digraphs, i.e., digraphs without self-arcs. We adopt the convention that information flows from vertex i to vertex j if $(i,j) \in \mathcal{E}$, and we call i an in-neighbor of j, and j an out-neighbor of i. A *walk* from a vertex i to a vertex j, denoted by w_{ij}, is a sequence $\{i_0, i_1, \ldots, i_m\}$, with $i_0 = i$ and $i_m = j$, in which each pair $(i_k, i_{k+1}) \in \mathcal{E}$ for all $k \in \{0, 1, \ldots, m-1\}$. A *path* corresponds to a walk in which all the vertices are pairwise distinct. A *cycle* is a walk in which there is no repetition of vertices other than the repetition of the starting and ending vertex. The *length* of a path/cycle/walk is defined to be the number of edges in that path/cycle/walk. A vertex $i \in \mathcal{V}$ is said to be a *root* of $\mathcal{G}$ if for any other vertex $j \in \mathcal{V}$, there exists a path from i to j. A digraph $\mathcal{G}$ with at least one root is a *rooted digraph*. A rooted digraph $\mathcal{G}$ without a cycle is *rooted acyclic*. If $\mathcal{G}$ is rooted acyclic, then there is a unique root. In general, a rooted digraph $\mathcal{G}$ can have multiple roots. All the roots then form a strongly connected subgraph $\mathcal{G}_R$. We call $\mathcal{G}_R$ the *root component* of $\mathcal{G}$. The digraph $\mathcal{G}$ is said to be *quasi-acyclic* if all the cycles of $\mathcal{G}$ are contained in the root component. In other words, if we condense $\mathcal{G}_R$ into a single vertex, then the resulting condensed digraph, denoted by $\mathcal{G}_c$, is rooted acyclic. A rooted acyclic digraph is a *directed tree* if every vertex, except the root, has a single in-neighbor. Every rooted digraph $\mathcal{G} = (\mathcal{V}, \mathcal{E})$ contains a directed tree $\mathcal{T} = (\mathcal{V}, \mathcal{E}')$, with the same vertex set, as its subgraph. We call $\mathcal{T}$ a *directed spanning tree*. Let $\mathcal{G}$ be a directed tree with i^* the root. The *depth* of a vertex i other than i^*, denoted by $\mathrm{dep}(i)$, is the length of the unique path from i^* to i. The depth of i^* is 0 by default. The *depth of* $\mathcal{G}$ is $\mathrm{dep}(\mathcal{G}) := \max_{v_i\in\mathcal{V}} \mathrm{dep}(i)$. For the given directed tree $\mathcal{G}$, we decompose the vertex set $\mathcal{V}$ as $\mathcal{V} = \cup_{l=0}^{\mathrm{dep}(\mathcal{G})} \mathcal{V}_l$, where $\mathcal{V}_l$ contains all the vertices of depth l. Let $\mathcal{G}$ be a rooted digraph. We define the depth of $\mathcal{G}$, denoted by $\mathrm{dep}(\mathcal{G})$, to be the maximal depth of a directed spanning tree $\mathcal{T}$ of $\mathcal{G}$.

2.2. Hybrid dynamical systems with random inputs

A stochastic hybrid dynamical systems (SHDS) with state $x \in \mathbb{R}^n$ and random input $v \in \mathbb{R}^m$ is characterized by the following set of equations:

$$x \in C, \qquad \dot{x} = f(x), \tag{4a}$$

$$x \in D, \qquad x^+ \in G(x, v^+), \quad v \sim \mu(\cdot), \tag{4b}$$

where the function $f : \mathbb{R}^n \to \mathbb{R}^n$, called the *flow map*, describes the continuous-time dynamics of the system; the set $C \subset \mathbb{R}^n$, called the *flow set*, describes the points in the space where x is allowed to evolve according to the differential equation (4a); $G : \mathbb{R}^n \times \mathbb{R}^m \rightrightarrows \mathbb{R}^n$, called the jump map, is a set-valued mapping that characterizes the discrete-time dynamics of the system; and $D \subset \mathbb{R}^n$, called the jump set, describes the points in the space where x is allowed to evolve according to the stochastic difference inclusion (4b). We use v^+ as a place holder for a sequence of independent, identically distributed (*i.i.d.*) input random variables $\{\mathbf{v_k}\}_{k=1}^{\infty}$ with probability distribution μ, derived from an abstract probability space $(\Omega, \mathcal{F}, \mathbb{P})$. General SHDS of the form (4) have been introduced and analyzed in Subbaraman and Teel (2016). In this paper we restrict our attention to SHDS that satisfy the following basic conditions:

Definition 1 (*Basic Conditions*)**.** A SHDS is said to satisfy the **basic conditions** if the following holds: (a) The sets C and D are closed, $C \subset \mathrm{dom}(f)$, and $D \subset \mathrm{dom}(G)$. (b) The function f is continuous. (c) The set-valued mapping $G : \mathbb{R}^n \times \mathbb{R}^m \rightrightarrows \mathbb{R}^n$ is locally bounded and the mapping $v \mapsto \mathrm{graph}(G(\cdot, v)) := \{(x,y) \in \mathbb{R}^n \times \mathbb{R}^n : y \in G(x,v)\}$ is measurable with closed values.

When the discrete-time dynamics (4b) do not depend on random inputs, the SHDS (4) is reduced to a standard deterministic HDS (Goebel et al., 2012):

$$x \in C, \qquad \dot{x} = f(x), \tag{5a}$$

$$x \in D, \qquad x^+ \in G(x). \tag{5b}$$

Solutions to hybrid systems (either stochastic (4) or deterministic (5)) are parameterized by both continuous- and discrete-time indices $t \in \mathbb{R}_{\geq 0}$ and $j \in \mathbb{Z}_{\geq 0}$. The index t increases continuously during flows (4a) or (5a), and the index j increases by one when a jump occurs via (4b) or (5b).

Of particular interest to us are solutions that have an unbounded time domain in *both* t and j directions. Such type of solution is maximal (i.e., its domain is not a proper subset of the domain of other solution) and non-Zeno (i.e., they do not have accumulation points in t). For a precise definition of maximal non-Zeno solutions x to HDS of the form (5) we refer the reader to Appendix B. Similarly, for a precise definition of maximal random solutions $\mathbf{x}_\omega$ to SHDS of the form (4) we refer the reader to Appendix C.

2.3. Stability and convergence notions

In this paper, we will use the following standard stability notion (Goebel et al., 2012) for deterministic HDS (5):

Definition 2. A HDS $\mathcal{H} := \{C, f, D, G\}$ is said to render a compact set $\mathcal{A}$ **uniformly globally asymptotically stable (UGAS)** if there exists a function $\beta \in \mathcal{KL}$ such that every solution x of (5) satisfies the bound

$$|x(t,j)|_{\mathcal{A}} \leq \beta(|x(0,0)|_{\mathcal{A}}, t+j),$$

for all $(t,j) \in \text{dom}(x)$. We say that $\mathcal{H}$ renders $\mathcal{A}$ **uniformly globally fixed-time stable (UGFxTS)** if, additionally, there exists a $\overline{T} > 0$ such that $\beta(|x(0,0)|_{\mathcal{A}}, t+j) = 0$ for all $t+j \geq \overline{T}$ and all $x(0,0) \in C \cup D$.

The UGAS stability property introduced in Definition 2 is standard in the analysis of hybrid dynamical systems, see Goebel et al. (2012, Chp. 3). On the other hand, the notion of UGFxTS is stronger, since it asks that every solution of the system should converge in finite time to the set $\mathcal{A}$, with a convergence time that can be upper bounded by a constant independent of the initial conditions. When C and D are compact, global fixed-time stability is equivalent to global finite-time stability.

To study the stability properties of SHDS of the form (4), we use the following definition borrowed from Teel (2013):

Definition 3. A SHDS (4) is said to render a compact set $\mathcal{A}$:

(a) **Uniformly Lyapunov stable in probability** if for each $\varepsilon > 0$ and $\rho > 0$ there exists a $\delta > 0$ such that for all $x_\omega(0,0) \in \mathcal{A} + \delta\mathbb{B}$, every maximal random solution $\mathbf{x}_\omega$ from $x_\omega(0,0)$ satisfies the inequality:

$$\mathbb{P}\Big(\mathbf{x}_\omega(t,j) \in \mathcal{A} + \varepsilon\mathbb{B}^\circ, \ \forall\, (t,j) \in \text{dom}(\mathbf{x}_\omega)\Big) \geq 1 - \rho. \tag{6}$$

(b) **Uniformly Lagrange stable in probability** if for each $\delta > 0$ and $\rho > 0$, there exists an $\varepsilon > 0$ such that the inequality (6) holds.

(c) **Uniformly globally attractive in probability** if for each $\varepsilon > 0$, $\rho > 0$ and $R > 0$, there exists a $\gamma \geq 0$ such that for all random solutions $\mathbf{x}_\omega$ with $x_\omega(0,0) \in \mathcal{A} + R\mathbb{B}$ the following holds:

$$\mathbb{P}\Big(\mathbf{x}_\omega(t,j) \in \mathcal{A} + \varepsilon\mathbb{B}^\circ, \forall\, t+j \geq \gamma, (t,j) \in \text{dom}(\mathbf{x}_\omega)\Big) \geq 1 - \rho.$$

System (4) is said to render a compact set $\mathcal{A} \subset \mathbb{R}^n$ **Uniformly Globally Asymptotically Stable in Probability (UGASp)** if it satisfies conditions (a), (b), and (c).

Definition 3 is a natural extension of Definition 2 to the stochastic domain. Moreover, under the Basic Conditions and certain causality assumptions on the solutions of the system, UGASp is a property that can be established by combining suitable Lyapunov functions and stochastic hybrid invariance principles (Subbaraman & Teel, 2016, Thm. 8). These tools will be instrumental in the analysis of our algorithms in the next sections.

3. Deterministic resetting algorithms

In this section we study how to construct deterministic BPRs that are scalable and that achieve robust global synchronization in PCOs over sparse networks.

3.1. Well-posed model for robust synchronization

We start by constructing suitable regularizations of discontinuous BPRs of the form (3). First, we recall that if all the agents are completely decoupled, then their dynamics are described by (1) and (2). When agents are coupled through a network, every agent i will send a pulse to its out-neighbors whenever τ_i reaches 1 and resets the value to 0 via (2). On the other hand, if agent j receives a pulse from its in-neighbor, then we assign the following set-valued BPR to the agent j:

$$\tau_j^+ \in \overline{\mathcal{P}}_j(\tau_j) := \begin{cases} \{0\} & \tau_j \in [0, r_j) \\ \{0,1\} & \tau_j = r_j \\ \{1\} & \tau_j \in (r_j, 1] \end{cases}, \tag{7}$$

where $r_j \in [0,1)$ is the tuning parameter. Each r_j partitions $[0,1]$ into two segments. For convenience, we call $r := [r_1; \ldots; r_N]$ a ***partition vector***.

Remark 1. As in Poveda and Teel (2019a) and Teel and Poveda (2015), the set-valued mapping $\overline{\mathcal{P}}_j : [0,1] \rightrightarrows \{0,1\}$ in Eq. (7) is generated as the outer semicontinuous hull[1] of the BPR (3) with forward map $F_j(\tau_j) = 1$ and backward map $B_j(\tau_j) = 0$. This regularization is used in the robustness analysis of discontinuous dynamical systems (Kellet & Teel, 2004), which will allow to establish suitable robustness results for synchronization dynamics.

We now model the dynamics of the agents, together with the BPRs (7), as a HDS of the form (5) with overall state $\tau = [\tau_1, \tau_2, \ldots, \tau_N]^\top$. Given a digraph $\mathcal{G}$ of N vertices, and a partition vector $r \in [0,1]^N$, we write the HDS as

$$\mathcal{H}(r, \mathcal{G}) := \{C, f, D, G\}, \tag{8}$$

with flow and jump sets given by

$$C := [0,1]^N \text{ and } D := \big\{\tau \in C : \max_{i \in \mathcal{V}} \tau_i = 1\big\}, \tag{9}$$

respectively; flow map and jump map given by

$$f(\tau) := \frac{1}{T} \cdot \mathbf{1}_N \quad \text{and} \quad G(\tau) := \overline{G^0(\tau)}, \tag{10}$$

respectively, where $\overline{G^0}$ is the outer-semicontinuous hull of the set-valued mapping $G^0 : [0,1]^N \rightrightarrows \mathbb{R}^N$ given by

$$G^0(\tau) := \Bigg\{ g \in \mathbb{R}^N : g_i = 0, \quad g_j \in \begin{Bmatrix} \overline{\mathcal{P}}_j(\tau_j), & (i,j) \in \mathcal{E} \\ \{\tau_j\}, & (i,j) \notin \mathcal{E} \end{Bmatrix}, \ \forall\, j \neq i \Bigg\}, \tag{11}$$

[1] See Appendix A for a precise definition of the outer semicontinuous hull of a mapping.

which is defined to be nonempty only when $\tau_i = 1$ for some $i \in \mathcal{V}$ and $\tau_j \in [0, 1)$ for $j \neq i$. Importantly, as in Poveda and Teel (2019a), by construction of the jump set and the jump map, when more than two agents satisfy the condition $\tau_i = 1$, their jumps will occur sequentially rather than in parallel. This behavior is induced on purpose to guarantee a suitable semi-continuous dependence on the initial conditions for the solutions of the system. Indeed, in order to capture the effect of arbitrarily small disturbances acting on the states of the PCOs, the synchronization model must guarantee that, for each initial condition $\tau_0 \in [0, 1]$, and each graphically convergent sequence of solutions $\{\tau^{(k)}\}_{k\in\mathbb{Z}_{\geq 0}}$ with components $\tau_i^{(k)}$ satisfying

$$0 \leq \tau_i^{(k)}(0,0) \leq \tau_{i+1}^{(k)}(0,0) \leq \cdots \leq \tau_{i+I}^{(k)}(0,0) < \tau_0, \tag{12}$$

for some $i \in \mathcal{V}$ and $I \in \mathbb{Z}_{>0}$, and

$$\lim_{k\to\infty} \tau_i^{(k)}(0,0) = \lim_{k\to\infty} \tau_{i+1}^{(k)}(0,0) = \cdots$$
$$\cdots = \lim_{k\to\infty} \tau_{i+I}^{(k)}(0,0) = \tau_0,$$

the sequence of solutions must graphically converge to a solution of the system starting from the set of initial conditions

$$\tau_i = \tau_{i+1} = \cdots = \tau_I = \tau_0. \tag{13}$$

This condition is particularly relevant for the case when $\tau_0 = 1$, since it implies that the states $\tau_i^{(k)}$ with initial conditions satisfying (12) are *sequentially* reset with smaller and smaller times between resets as $k \to \infty$. Thus, in the limiting case (13), all agents must reset their states but the resets must occur *sequentially*. Since no order is specified for the sequential jumps, and there is no reason to give priority to one agent over the other, any robust model of PCOs must take into account all the possible trajectories induced by the $N!$ different resetting orders that can emerge from condition (13) with $\tau_0 = 1$, $i = 1$, and $I = N$.

Remark 2. The construction of G suggests that studying the individual behavior of every possible solution of the system becomes intractable as N increases. In order to address this issue, in this paper we will use Lyapunov stability theory to analyze the qualitative behavior of *every* possible solution of the system *from any initial condition in* $[0, 1]^N$.

The following fact follows directly from the construction:

Lemma 1. *For every partition vector r and every digraph $\mathcal{G}$, the HDS $\mathcal{H}(r, \mathcal{G})$ introduced in (8) satisfies the basic conditions.*

We aim to characterize pairs $(r, \mathcal{G})$ that make the corresponding HDS $\mathcal{H}(r, \mathcal{G})$ well behaved (non-Zeno behavior) and, moreover, render the following compact set UGAS:

$$\mathcal{A}_s := \{\mu \mathbf{1}_N \mid \mu \in [0, 1]\} \cup \{0, 1\}^N. \tag{14}$$

It should be clear that if the state τ belongs to $\mathcal{A}_s$, then the network flows synchronously. For convenience, we introduce the following definition:

Definition 4. Let $\mathcal{A}_s$ be the compact set in (14). Let $r \in [0, 1)^N$ be a partition vector and $\mathcal{G}$ be a digraph of N vertices. The pair $(r, \mathcal{G})$ is a **sync-pair** if

(a) For every initial condition in $C \cup D$ there exists a non-trivial solution to $\mathcal{H}(r, \mathcal{G})$, and each solution has an unbounded time domain and it is uniformly non-Zeno (see Goebel et al., 2012, Prop. 6.35-(a));
(b) The HDS $\mathcal{H}(r, \mathcal{G})$ renders UGAS the set $\mathcal{A}_s$.

While the stability analysis of the set $\mathcal{A}_s$ will be highly dependent on the communication digraph $\mathcal{G}$ and the partition vector r, the following Lemma will be instrumental in satisfaction of item (a) in Definition 4.

Lemma 2. *Consider the HDS $\mathcal{H}(r, \mathcal{G})$. For any partition vector $r \in (0, 1)^N$ and any digraph $\mathcal{G}$ we have that item (a) in Definition 4 holds, and the number of jumps in any interval of length T is bounded above by $\ell^* := N(\lfloor 1/\underline{r} \rfloor + 1)$ where $\underline{r} := \min_{i\in\mathcal{V}} r_i$.*

Proof. Let $\mathcal{G}$ be given, and let $r \in (0, 1)^N$. Since the HDS $\mathcal{H}(r, \mathcal{G})$ satisfies the basic conditions, and since $f(\tau) > 0$ for all $\tau \in [0, 1)^N$, by Goebel et al. (2012, Prop. 6.10) there exists at least one non-trivial solution from every initial condition $\tau(0, 0) \in C \cup D$. Since the flow map is globally Lipschitz and the flow set is compact, every solution τ does not exhibit finite escape times. Moreover, since $G(D) \subset C \cup D$ solutions cannot stop due to jumps. Thus, by Goebel et al. (2012, Prop. 6.10) every solution τ is complete, i.e., it has an unbounded time domain. To show absence of Zeno-behavior, it suffices to rule out the existence of discrete solutions to system $\mathcal{H}(r, \mathcal{G})$ (Goebel et al., 2012, Prop. 6.35). Suppose by contradiction that there exists a maximal solution τ satisfying $\tau(0, j) \in D$ for all $j \in \mathbb{Z}_{\geq 0}$. This implies that for all $j \in \mathbb{Z}_{\geq 0}$ there exists some $i^* \in \mathcal{V}$ such that $\tau_{i^*}(0, j) = 1$. By construction of the dynamics, and without loss of generality, we will have that $\tau_{i^*}(0, j + 1) = 0$, which implies that agent i^* cannot trigger further jumps. This argument can be repeated at most $N - 1$ consecutive times, after which all agents would satisfy $\tau_i \neq 1$, i.e., $\tau(0, j + N) \notin D$, which contradicts the original assumption.

We now establish the upper bound. Note that if an agent i hits 1 and jumps at a certain hybrid time (t, j) (so that $\tau_i(t, j+1) = 0$), then the least time required by the agent i to hit again the value 1 is to first flow for $r_i T$ seconds and, then, to have one of its in-neighbors to hit 1 and trigger it. This implies that the number of times the agent i can hit 1 during the period $[t, t+T]$ is bounded above by $(1/r_i + 1)$ and, hence, $\lfloor 1/r_i \rfloor + 1$. Finally, the number of jumps of the entire network during the period $[t, t + T]$ is equal to the number of times N agents hit 1 during the same period, we conclude that the number of jumps is bounded above by $\sum_{i=1}^{N} (\lfloor 1/r_i \rfloor + 1) \leq N(\lfloor 1/\underline{r} \rfloor + 1)$. ■

Remark 3. Note that the conditions of Lemma 2 rule out the case where there is a certain r_i taking the value 0. We do so because it could generate Zeno solutions. Specifically, if two agents i and j with bi-directional links have their tuning parameters r_i and r_j equal to 0, there exists a solution in which agent i resets τ_i from 1 to 0, triggering agent j to update τ_j to 1, which will be followed by an update of the form $\tau_j^+ = 0$, which in turn will trigger agent i to update its state τ_i to 1. The process repeats infinitely, generating a purely discrete-time solution. In order to avoid this behavior, we will introduce later in Theorem 2 a class of digraphs for which Zeno solutions do not emerge even when $r = 0$.

An advantage of formulating the closed-loop system of PCOs as HDS satisfying the basic conditions is that we can leverage existing theoretical tools to establish suitable robustness results. Specifically, we have the following fact:

Lemma 3. *If $(r, \mathcal{G})$ is a sync-pair, then there exists a $\beta \in \mathcal{KL}$ such that for each $\nu > 0$ there exists $e^* > 0$ such that for all measurable functions $e_i : \text{dom}(e) \to \mathbb{R}^N$, $i \in \{1, 2, \ldots, 6\}$, satisfying $\sup_{t+j\geq 0} |e_i(t, j)| \leq e^*$, every solution of the perturbed HDS $\mathcal{H}(r, \mathcal{G}) + e$, given by*

$$\tau + e_1 \in C, \qquad \dot{\tau} = f(\tau + e_2) + e_3, \tag{15a}$$

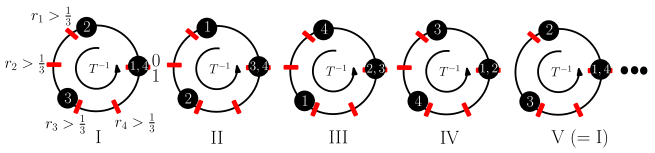

Fig. 1. Illustration of the counter example in the proof of item (b), Proposition 1 for $N = 4$. When $r_i > 1/3$ for all i, there exists a solution, shown in the figure, which repeats its initial condition infinitely often and can never achieve synchronization.

$$\tau + e_4 \in D, \qquad \tau^+ \in G(\tau + e_5) + e_6, \tag{15b}$$

satisfies the bound $|\tau(t,j)|_{\mathcal{A}_s} \leq \beta(|\tau(0,0)|_{\mathcal{A}_s}, t+j) + \nu$, *for all* $(t,j) \in \mathrm{dom}(\tau)$.

Proof. The result follows directly from item (b) of Definition 4, the compactness of $\mathcal{A}_s$, C, and D; the fact that $\mathcal{H}(r,\mathcal{G})$ is well posed, and the application of Goebel et al. (2012, Lemma 7.20). ■

3.2. Scalability issue and negative results

We start by presenting a known result established in Teel and Poveda (2015, Thm. 1) and Poveda and Teel (2019a, Prop. 1):

Lemma 4. *Let* $r \in (0, 1/N)^N$ *and* $\mathcal{G}$ *be a strongly connected digraph. Then,* $(r,\mathcal{G})$ *is a sync-pair. Moreover, the set* $\mathcal{A}_s$ *is UGFxTs. Every maximal solution* τ *satisfies* $|\tau(t,j)|_{\mathcal{A}_s} = 0, \quad \forall\ t \geq T^* := T$, *with* $(t,j) \in \mathrm{dom}(\tau)$.

Remark 4. Although Lemma 4 is a positive result, the condition $r \in (0, 1/N)^N$ for strongly connected digraphs causes the scalability issue; indeed, since each r_i is upper bounded by a term of order $\mathcal{O}(\frac{1}{N})$, the partition $[0, r_j)$ in (7) associated with each agent vanishes as $N \to \infty$. Moreover, if the size of the network is dynamic, then, in order to achieve fixed-time synchronization, one would need to persistently re-tune the parameters r_i of existing agents. Some existing works, such as Nishimura and Friedman (2011, 2012), have presented scalable algorithms with partition parameters $r_i = \frac{1}{2}$ for all $i = 1, \ldots, N$, but the synchronization results are only local or almost global. Other relevant works on global synchronization are restricted to specific digraphs, such as bidirectional connected graphs (Nunez et al., 2015b), strongly rooted graphs (Nunez et al., 2016), and bidirectional chains (Gao & Wang, 2019).

By taking a closer look at the proof of Lemma 4, we can relax slightly the condition by requiring that $r \in (0, 1/N-1)^N$. The trade-off is that the convergence time will be doubled as $2T$. However, such relaxation is still insufficient for fixing the scalability issue. Whether or not the condition can further be relaxed for some particular digraph is unknown. Nevertheless, we present an impossibility result for the family of strongly connected digraphs.

Proposition 1. *The following holds for the HDS* $\mathcal{H}(r,\mathcal{G}) := \{C, f, D, G\}$ *given by (8):*

(a) For every strongly connected digraph $\mathcal{G}$, *and every* $r \in (0, \frac{1}{N-1})^N$, *the pair* $(r,\mathcal{G})$ *is a sync-pair. Every maximal solution* τ *satisfies* $|\tau(t,j)|_{\mathcal{A}_s} = 0, \quad \forall\ t \geq T^* := 2T$, *with* $(t,j) \in \mathrm{dom}(\tau)$.

(b) For any $N \geq 3$, *there exists a strongly connected digraph* $\mathcal{G}$ *on* N *vertices such that for any* $r \in (\frac{1}{(N-1)}, 1)^N$, *the pair* $(r,\mathcal{G})$ *is not a sync-pair.*

Proof. We first show the existence of a uniformly bounded time $t^* \geq 0$ such that every solution of $\mathcal{H}(r,\mathcal{G})$ satisfies $\tau(t^*,0) \in D$ for any $r \in [0,1)^N$ and any digraph $\mathcal{G}$. Indeed, let $r \in [0,1)^N$ and $\mathcal{G}$ be given, and consider a solution of $\mathcal{H}(r,\mathcal{G})$. Let $\tau(0,0) \in C \backslash D$, otherwise there is nothing to prove. Then, it must be the case that $\tau_i(0,0) \in [0,1)$ for all $i \in \mathcal{V}$. By the construction of the flow map f in (10), it follows that during flows the solutions satisfy $\tau_i(t,j) = \frac{1}{T}(t - t_j) + \tau_i(t_j, j)$ for all $i \in \mathcal{V}$, where $t_j := \inf\{t \geq 0 : (t,j) \in \mathrm{dom}(\tau)\}$. Since the function is increasing in t, setting $j = 0$ and $t_j = 0$, there must exist $i^* \in \mathcal{V}$ and $t^* \geq 0$ such that $\tau_{i^*}(t^*, 0) = 1$. In turn, this implies

$$t^* = T(1 - \tau_{i^*}(0,0)) \leq T, \tag{16}$$

for all $\tau_i \in [0,1)$. Now, to establish item (a), note that by Lemma 2 every solution of the system is complete and uniformly non-Zeno. To show UGAS of $\mathcal{A}_s$, we now consider a suitable Lyapunov function $V : [0,1]^N \to \mathbb{R}_{\geq 0}$ defined as follows: First, pick two agents next to each other on the unit circle; next, use these two agents as the two endpoints of the arc that includes all the other agents in the circle (points 0 and 1 are identified to be the same point); then, define the Lyapunov function V to be the minimum of lengths of all such arcs (there are N such arcs). Note that this function is positive definite with respect to $\mathcal{A}_s$, and by construction V satisfies $0 \leq V(\tau(0,0)) \leq 1 - \frac{1}{N}$ for every possible initial condition $\tau(0,0) \in [0,1]^N$. Moreover, since during flows the function V does not change, and during jumps the function V cannot increase, it follows that the bound $V(\tau(t,j)) \leq 1 - \frac{1}{N}$ holds for all solutions τ of the HDS $\mathcal{H}(r,\mathcal{G})$. Additionally, by Eq. (16) we know that every solution will experience a jump at the hybrid time $(t^*, 0)$, triggered by at least one agent $i^* \in \mathcal{V}$ satisfying $\tau_{i^*} = 1$. Since the digraph is strongly connected, and the update rule (7) is binary, there exists at least one agent j^* that is an out-neighbor of agent i^* such that $\tau_{j^*}(t^*, 1) \in \{0, 1\}$. Therefore, agents i^* and j^* are now at the same position on the unit circle, and it follows that $0 \leq V(\tau(t^*, 1)) \leq 1 - \frac{1}{N-1}$. From this point, by using the same arguments that lead to Eq. (16), the system can stay in the flow set for at most T seconds, which implies the existence of an agent i^{**} and a time $t^{**} > 0$ such that $\tau_{i^{**}}(t^{**}, 1) = 1$. Since $V(\tau(t^{**}, 1)) \leq 1 - \frac{1}{N-1}$ still holds, it follows that necessarily $\tau_i \geq \frac{1}{N-1}$ for all $i \in \mathcal{V}$, and since the tuning parameters of all agents satisfy $r_i \in (0, \frac{1}{N-1})$, it follows that $\tau_i \in (r_i, 1]$ for all $i \in \mathcal{V}$, and by (7) and the fact that the digraph is strongly connected, the system will experience $N-1$ consecutive jumps, after which $\tau_i(t^{**}, j^*) = 0$ for all $i \in \mathcal{V}$. This establishes finite-time synchronization of the network with $t^{**} \leq 2T$, which, in turn, implies that there is no complete solution that keeps the Lyapunov function V in a non-zero level set. By the hybrid invariance principle (Goebel et al., 2012, Thm. 8.8) we conclude UGAS of $\mathcal{A}_s$. Finally, note that since every solution is uniformly non-Zeno, and the set of initial conditions is compact, there exists $j^* > 0$ such that the HDS will experience at most j^* jumps in any continuous-time interval of length $2T$. Therefore, the set $\mathcal{A}_s$ is actually UGFxTS with $\overline{T} = 2T + j^*$.

To prove item (b), it suffices to consider a counter-example for an arbitrary $N \geq 3$. Consider the cycle digraph having $N \geq 3$ vertices (see Fig. 1 for illustration). Let $r \in (\frac{1}{N-1}, 1)^N$ be an arbitrary partition vector. Without loss of generality we take $T = 1$. Choose the initial conditions for the agents as follows (for convenience, we will omit arguments of τ):

$$\tau_1 = \tau_N = 0 \ \text{ and } \ \tau_i = \frac{i-1}{N-1}, \ \forall\, i \in \{2, \ldots, N-1\}. \tag{17}$$

From this initialization, the system will flow for $\frac{1}{N-1}$ seconds, until the states of the agents satisfy $\tau_1 = \tau_N = \frac{1}{N-1}$ and $\tau_i = \frac{i}{N-1}$, $\forall\ i \in \{2, \ldots, N-1\}$, which implies that agent $(N-1)$ will be reset to zero and also trigger its out-neighbor N. Because $r_N > \frac{1}{N-1}$, agent N will reset its state to zero without triggering

its out-neighbor. Thus, the states of the agents are updated as follows: $\tau_{N-1} = \tau_N = 0$ and $\tau_i = \frac{i}{N-1}$, $\forall\, i \in \{1, \ldots, N-2\}$. The system will then flow again. Similarly, after $\frac{1}{N-1}$ seconds, the state of agent $(N-2)$ will reach one and immediately be reset to zero. Meanwhile, agent $(N-2)$ triggers its out-neighbor $(N-1)$. Because $r_{N-1} > \frac{1}{N-1}$, agent $(N-1)$ resets its state to zero. The states of the agents are thus updated as follows: $\tau_{N-2} = \tau_{N-1} = 0$ and $\tau_i = \frac{(i+1) \bmod N}{N-1}$, for all $i \in \{1, \ldots, N-3, N\}$. Proceeding with this system dynamics for another $\frac{N-2}{N-1}$ seconds, we will return to the initial condition (17), which implies that the agents can never reach synchronization. ■

Although the proof of the negative result of Proposition 1 is built upon cycle digraphs, there are other strongly connected digraphs that also have the scalability issue. However, a complete characterization of these digraphs remains open.

To fix the scalability issue, we consider below digraphs beyond the strongly connected ones. We start with the following necessary condition:

Proposition 2. *If $(r, \mathcal{G})$ is a sync-pair, then $\mathcal{G}$ is rooted.*

Proof. We apply strong component decomposition (see, for example, Chen, Belabbas, & Başar, 2017) to $\mathcal{G}$ and obtain strongly connected subgraphs $\mathcal{G}_l = (\mathcal{V}_l, \mathcal{E}_l)$, for $l = 1, \ldots, k$, where the subsets $\mathcal{V}_l$ form a partition of $\mathcal{V}$. A subgraph $\mathcal{V}_l$ is said to be a leading strong component if for any $v_j \in \mathcal{V} \backslash \mathcal{V}_l$ and any $v_i \in \mathcal{V}_l$, (i, j) is not an edge of $\mathcal{G}$. If a digraph $\mathcal{G}$ is not rooted, then it has at least two leading components. Without loss of generality, we assume that $\mathcal{G}_1$ and $\mathcal{G}_2$ are two leading components. Because a leading component does not have incoming neighbors, its dynamics are completely decoupled from the others. In particular, the dynamics of components $\mathcal{G}_1$ and $\mathcal{G}_2$ are independent of each other. Thus, the overall system cannot achieve synchronization from all initial conditions. ■

Conversely, we can ask whether for any given rooted digraph $\mathcal{G}$, there is a partition vector r such that $(r, \mathcal{G})$ is a sync-pair? The following result provides a negative answer:

Proposition 3. *There exists a rooted digraph $\mathcal{G}$ on N vertices, for $N \geq 3$, such that for any $r \in (0, 1)^N$ the pair $(r, \mathcal{G})$ is not a sync-pair.*

Proof. The proof is constructive. Let us consider the digraph shown in Fig. 2, which is obtained by adding the edge $(3, 2)$ to a path digraph. Pick an arbitrary $r \in (0, 1)^N$, and we will need to exhibit an initial condition for which the system cannot reach synchronization. By the structure of the digraph, the dynamics of agents $4, \ldots, N$ do not affect the dynamics of agents 1, 2, and 3. Thus, it suffices to find initial conditions for the first three agents for which they cannot reach synchronization (the initial conditions for the remaining agents can then be arbitrary). This is done below and illustrated in Fig. 2.

Without loss of generality we consider $T = 1$. Define $\tau_{i,0} := \tau_i(0, 0)$ for $i \in \{1, 2, 3\}$. We consider two scenarios: (a) $r_2 \leq 0.5$; and (b) $r_2 > 0.5$.

Scenario (a): Choose $\tau_{2,0}$ such that $1 - r_3 < \tau_{2,0} \leq 1$. Choose $\tau_{1,0}$ such that

$$\max\{0, \tau_{2,0} - r_2\} < \tau_{1,0} < \tau_{2,0}, \tag{18}$$

and choose $\tau_{3,0}$ such that

$$0 < \tau_{3,0} < \min\{\tau_{1,0}, \tau_{2,0} - (1 - r_3)\}. \tag{19}$$

Note that this initialization satisfies $1 > \tau_{2,0} > \tau_{1,0} > \tau_{3,0} > 0$. Following the hybrid dynamics we obtain the following sequence of events: Agents flow for $1 - \tau_{2,0}$ seconds, until the system satisfies the condition $\tau_1 = \tau_{1,0} + (1 - \tau_{2,0})$, $\tau_2 = 1$, $\tau_3 = \tau_{3,0} + (1 - \tau_{2,0})$. By the right hand side of inequality (19) we obtain that $\tau_3 < r_3$, and the states will jump as $\tau_1^+ = \tau_1$, $\tau_2^+ = 0$ and $\tau_3^+ = 0$. Following this jump, the system will flow for $1 - (\tau_{1,0} + (1 - \tau_{2,0}))$ seconds, until the system satisfies the following condition:

$$\tau_1 = 1, \quad \tau_2 = \tau_{2,0} - \tau_{1,0}, \quad \tau_3 = \tau_{2,0} - \tau_{1,0}. \tag{20}$$

By the left hand side of inequality (18) we have $\tau_2 < r_2$. Therefore, the system will jump as $\tau_1^+ = 0$, $\tau_2^+ = 0$ and $\tau_3^+ = \tau_3$. Following this jump, the system will flow for $1 - \tau_{2,0} + \tau_{1,0}$ seconds, until the following condition holds:

$$\tau_1 = \tau_{1,0} + (1 - \tau_{2,0}), \quad \tau_2 = \tau_{1,0} + (1 - \tau_{2,0}), \quad \tau_3 = 1. \tag{21}$$

Since $r_2 \leq 0.5$, it follows that $r_2 \leq 1 - r_2$ and $\tau_{0,2} - r_2 \geq \tau_{2,0} - (1 - r_2)$. Therefore, using again the left hand side of inequality (18) we obtain that $\tau_2 > r_2$ in (27). Thus, the system will jump as $\tau_1^+ = \tau_1$, $\tau_2^+ = 1$ and $\tau_3^+ = 0$. At this point the system will jump again as $\tau_1^+ = \tau_1$, $\tau_2^+ = 0$ and $\tau_3^+ = 0$. After $1 - \tau_1$ seconds of flow, the system will satisfy the condition

$$\tau_1 = 1, \quad \tau_2 = \tau_{2,0} - \tau_{1,0}, \quad \tau_3 = \tau_{2,0} - \tau_{1,0}, \tag{22}$$

which is the same state described in (20), i.e., the system has entered a periodic cycle which includes points outside the set $\mathcal{A}$.

Scenario (b): Choose $\tau_{2,0}$ such that $\max\{1 - r_3, 1 - r_2\} < \tau_{2,0} \leq 1$ holds. Choose $\tau_{1,0}$ such that

$$\max\{0, \tau_{2,0} - r_2\} < \tau_{1,0} < \tau_{2,0} - (1 - r_2). \tag{23}$$

This choice is always possible given that $r_2 > 0.5$. Choose $\tau_{3,0}$ such that

$$0 < \tau_{3,0} < \min\{\tau_{1,0}, \tau_{2,0} - (1 - r_3)\}. \tag{24}$$

Note that this initialization is always feasible and satisfies $1 > \tau_{2,0} > \tau_{1,0} > \tau_{3,0} > 0$. Following the hybrid dynamics we obtain the following sequence of events: Agents flow for $1 - \tau_{2,0}$ seconds until the states satisfy $\tau_1 = \tau_{1,0} + (1 - \tau_{2,0})$, $\tau_2 = 1$, $\tau_3 = \tau_{3,0} + (1 - \tau_{2,0})$. By the right hand side of inequality (24) we obtain that $\tau_3 < r_3$, and the states will jump as $\tau_1^+ = \tau_1$, $\tau_2^+ = 0$ and $\tau_3^+ = 0$. Following this jump, the system will flow for $\tau_{2,0} - \tau_{1,0}$ seconds, until the system satisfies the following condition:

$$\tau_1 = 1, \quad \tau_2 = \tau_{2,0} - \tau_{1,0}, \quad \tau_3 = \tau_{2,0} - \tau_{1,0}. \tag{25}$$

By the left hand side of inequality (23) we have $\tau_2 < r_2$. Therefore, the system will jump as $\tau_1^+ = 0$, $\tau_2^+ = 0$ and $\tau_3^+ = \tau_3$. Following this jump, the system will flow for $1 - \tau_{2,0} + \tau_{1,0}$ seconds, until the following condition holds:

$$\tau_1 = \tau_{1,0} + (1 - \tau_{2,0}), \quad \tau_2 = \tau_{1,0} + (1 - \tau_{2,0}), \quad \tau_3 = 1. \tag{26}$$

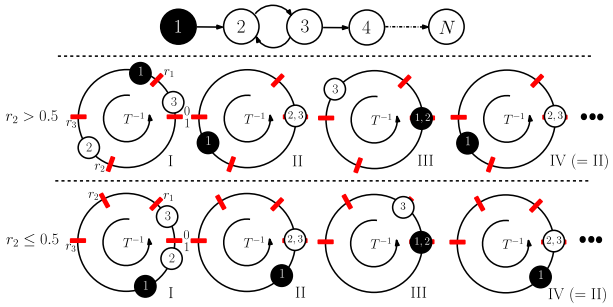

Fig. 2. Illustration of the counter-example in the proof of Proposition 3. Top: Rooted digraph with vertex 1 the root and a 2-cycle form by vertices 2 and 3. Center: Problematic solution for case $r_2 > 0.5$. Bottom: Problematic solution for $r_2 \leq 0.5$.

By the right-hand side of (23) we obtain that $\tau_2 < r_2$ in (26). Thus, the system will jump as $\tau_1^+ = \tau_1$, $\tau_2^+ = 0$ and $\tau_3^+ = 0$. After $1-\tau_1$ seconds of flow, the system will satisfy the condition

$$\tau_1 = 1, \;\; \tau_2 = \tau_{2,0} - \tau_{1,0}, \;\; \tau_3 = \tau_{2,0} - \tau_{1,0}, \tag{27}$$

which is the same state (25), i.e., the system has entered a periodic cycle which includes points outside the set $\mathcal{A}_s$.

Since scenarios (a) and (b) cover every possible choice of $r \in (0,1)^N$, and for any choice we found a solution that does not converge to $\mathcal{A}_s$, the pair $(r, \mathcal{G})$ is not a sync-pair for any partition vector $r \in (0,1)^N$. ■

Remark 5. It is well known that for standard consensus dynamics in $\mathbb{R}^N$, the digraph $\mathcal{G}$ being rooted is a necessary and sufficient condition for state synchronization. Moreover, finite-time consensus in $\mathbb{R}^N$ can also be achieved under the same graphical condition (Wang, Yu, Ren, & Lu, 2019). Proposition 2 shows that, in order to achieve synchronization, the connectivity requirement for the network of PCOs is completely different from the one for the standard consensus dynamics.

3.3. Positive result on rooted acyclic digraphs

In this subsection, we focus on a special class of rooted digraphs, namely rooted acyclic digraphs (see Fig. 3 for illustration). We will show that for every such digraph $\mathcal{G}$ and for every partition vector $r \in [0,1)^N$, the tuple $(r, \mathcal{G})$ is a sync-pair. In particular, the choice of r can be made independent of the size N of the digraph. We formulate the result in the following theorem:

Theorem 1. *For any rooted acyclic digraph $\mathcal{G}$ and any $r \in (0,1)^N$, $(r, \mathcal{G})$ is a sync-pair. Moreover, every maximal solution τ satisfies*

$$|\tau(t,j)|_{\mathcal{A}_s} = 0, \quad \forall \;\; t \geq T^* := (\text{dep}(\mathcal{G}) + 1)T, \tag{28}$$

with $(t,j) \in \text{dom}(\tau)$.

Proof. We consider again the Lyapunov function $V : [0,1]^N \to \mathbb{R}_{\geq 0}$ defined as the infimum of all the arcs that touch all agents on the unit circle, where the points 0 an 1 are identified to be the same. By Teel and Poveda (2015), this Lyapunov function satisfies the following properties: (i) It is positive definite with respect to the compact set (14). (ii) It remains constant during flows because all the oscillators have the same frequency $\frac{1}{T}$. (iii) It does not increase at jumps since jumps never increase the number of distinct points occupied by the agents. We claim that there is no maximal solution of the HDS $\mathcal{H}(r, \mathcal{G})$ that keeps V equal to a non-zero constant. We show this by establishing fixed-time synchronization. Let $\tau(0,0) \in [0,1]^N$ and τ be a solution of the HDS (8). Recall that $\mathcal{V}_l$ defines all vertices/agents of depth l. Since the digraph is rooted acyclic, no agent can influence the unique root agent, and without loss of generality, we assume that τ_1 corresponds to the root agent, i.e., $\mathcal{V}_0 = \{1\}$. Based on this, we proceed to establish a uniform upper bound on the amount of hybrid time that can pass before the Lyapunov function is exactly equal to zero. We establish the fact by induction on the depth l of the vertices of $\mathcal{G}$.

- *Base Case $l = 1$:* In at most T seconds of flow, τ will satisfy $\tau_1 = 1$, and agent 1 will trigger all the vertices in $\mathcal{V}_1$ to either jump to 0 or 1. Thus, based on r, there will exist a partition of $\mathcal{V}_1$ that is defined by the index sets (I', I'', I''') such that: (i) for all $i' \in I'$, $\tau_{i'} > r_i$ (the agents i' will jump to 1 and trigger $\mathcal{V}_2$); (ii) for all $i'' \in I''$, $\tau_{i''} < r_i$ (the agents i'' will jump to 0 and flow for at most T seconds to trigger $\mathcal{V}_2$); (iii) for all $i''' \in I'''$, $\tau_{i'''} = r_i$ (the agents i''' will have a set-valued jump $\{0,1\}$. If the agent jumps to 1, it will follow (i), otherwise, it will follow (ii)).

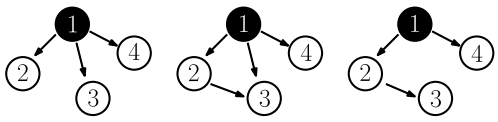

Fig. 3. Rooted acyclic digraphs. Left: Depth = 1; Center: Depth = 2; Right: Depth = 2. Black vertex indicates the root.

Note that after the first jump, $\mathcal{V}_0$ synchronizes with $\mathcal{V}_1$ within at most $2T$ seconds and remains synchronized since $\mathcal{V}_1$ does not influence $\mathcal{V}_0$ by the acyclic property of the digraph.

- *Induction Step:* Suppose that agents $\{\mathcal{V}_0, \mathcal{V}_1, \ldots, \mathcal{V}_k\}$ synchronize in at most $(k+1)T$ seconds, where $k < \text{dep}(\mathcal{G})$. Since the digraph does not have a cycle, and the root/agent has a path to all the agents, we have that agents $\mathcal{V}_k$ only influence agents $\mathcal{V}_{k+1}$ and cannot affect already synchronized agents $\mathcal{V}_l$, for $0 \leq l \leq k-1$. Thus, agents $\{\mathcal{V}_0, \mathcal{V}_1, \ldots, \mathcal{V}_{k+1}\}$ synchronize in at most $(k+2)T$ seconds. Therefore, the agents $\{\mathcal{V}_0, \mathcal{V}_1, \ldots, \mathcal{V}_{\text{dep}(\mathcal{G})}\}$ synchronize in at most $(\text{dep}(\mathcal{G}) + 1)T$ seconds and remain synchronized after that, i.e., they occupy the same position on the unit circle for all $(t,j) \in \text{dom}(\tau)$.

Furthermore, by Lemma 2, the above arguments imply that $V(\tau(t,j)) = 0$ for all $(t,j) \in \text{dom}(\tau)$ such that $t + j \geq (\text{dep}(\mathcal{G}) + 1)(T + N(\lfloor 1/r \rfloor + 1)) =: \overline{T}$. Since τ was arbitrary, we have established that there is no solution of the HDS that keeps the Lyapunov function in a non-zero level set. We can now directly establish UGAS of the HDS $\mathcal{H}(r, \mathcal{G})$ with respect to the compact set $\mathcal{A}_s$ by using the Hybrid Invariance Principle (Sanfelice, Goebel, & Teel, 2007). Absence of purely or eventually discrete-time solutions follows by Lemma 2. This completes the proof of the Theorem. ■

For the special case where $r = 0_N$, we have the following:

Theorem 2. *A pair $(0_N, \mathcal{G})$ is a sync-pair if and only if $\mathcal{G}$ is rooted acyclic. In this case, (28) holds with $T^* := T$.*

Proof. *Sufficiency:* First, we show that every solution is non-Zeno. Indeed, by construction, Zeno behavior can only occur if there exists a solution τ that remains in the jump set D for all $(t,j) \in \text{dom}(\tau)$. In order to remain in D, for such solution there must exist an agent i satisfying $\tau_i(0,0) = 1$, and an agent j and a path from i to j and from j to i. Otherwise, after at most N jumps all other agents have already been triggered to 0 and $\tau \notin D$. However, since by assumption the digraph is acyclic, there are no two vertices i, j that have a path from each other. Thus, at most N consecutive jumps can occur in the system until the state satisfies $\tau = 0_N \in C \backslash D$. To show UGAS, note that since the root agent is not affected by any other vertex, for every solution of the HDS $\mathcal{H}(0_N, \mathcal{G})$ there exists $(t^*, j^*) \in \text{dom}(\tau)$ with $t^* \leq T$ and $j^* \leq N$ such that the state of the root vertex v^* satisfies $\tau_{v^*}(t^*, j^*) = 1$. Based on this, we claim that every solution τ will satisfy $V(\tau(t,j)) = 0$ for all $(t,j) \in \text{dom}(\tau)$ such that $t + j \geq T + 2N$, where V is the same Lyapunov function used in the proof of Theorem 1. We prove the claim by considering the two possible cases: (a) $t^* > 0$; and (b) $t^* = 0$. Suppose that case (a) holds; then, since $t^* > 0$, whenever $\tau_{v^*}(t^*, j^*) = 1$ and $\tau_{v^*}(t^*, j^* + 1) = 0$, every other neighbor vertex j satisfying $\tau_j(t^*, j^*) \in (0,1]$ will satisfy $\tau_j(t^*, j^* + 1) = 1$. Similarly, since $r = 0_N$, every neighbor vertex j satisfying $\tau_j(t^*, j^*) = 0$ will satisfy $\tau_j(t^*, j^* + 1) \in \{0,1\}$. Moreover, since $t^* > 0$, every such neighborhood satisfying $\tau_j(t^*, j^*) = 0$ must have already reset its own state, thus also triggering its own neighbors to update their states following the same rules described above. Since the digraph is rooted acyclic, and no agent can trigger the root node

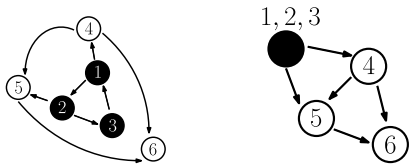

Fig. 4. (a) Quasi-acyclic digraph $\mathcal{G}$. (b) Condensed digraph $\mathcal{G}_c$.

v^*, this process will repeat at most $N-1$ times, until all agents have been triggered and reset to $\tau_j = 0$. Thus, the same Lyapunov function used in the proof of Theorem 1 allows us to establish UGAS of $\mathcal{A}$ via the hybrid invariance principle. If case (b) holds, note that after at most T seconds the root vertex v^* would satisfy $\tau_{v^*} = 1$, and at this point case (a) will hold.

Necessity: It follows from the previous observation that whenever i^* is the vertex of a cycle $\mathcal{C}$, and $r = 0_N$, the condition $\tau_{i^*}(0,0) = 1$ will trigger sequentially all the vertices of the cycle until every vertex $k \in \mathcal{C}$ satisfies $\tau_k \in \{0,1\}$, with at least one vertex $j \in \mathcal{C}$ satisfying $\tau_j = 1$. By definition of cycle, the vertex j will trigger at least one vertex k satisfying $\tau_k = 0$, generating the update $\tau_k^+ = 1$. This process repeats infinitely times generating a discrete solution. Therefore, if $(0_N, \mathcal{G})$ is a sync-pair, the digraph $\mathcal{G}$ cannot have cycles. ■

Theorems 1 and 2 highlight two novel properties of PCOs with digraphs and resetting BPRs of the form (7): First, *robust fixed-time global* synchronization can be achieved in a *scalable* way for any network characterized by a rooted acyclic digraph. Indeed, in this case the bound on the parameter r_i of each agent is of order $\mathcal{O}(1)$; Second, for this kind of digraphs, the synchronization can be accelerated by the parameter choice $r = 0_N$, which, as noted in Remark 3, is prohibited if the digraphs have cycles. The results also highlight the role of the depth of the digraph in the convergence time of the hybrid dynamics. Finally, by the results of Lemma 3, the synchronization properties established in Theorems 1 and 2 are preserved for the perturbed HDS (15), which allow us to consider small delays and drifts on the PCO's states.

Remark 6. While Theorems 1 and 2 do not cover the case where $r_i = 0$ only for *some* agents of the network, it is clear from the proof of Theorem 2 that if $\mathcal{G}$ is rooted acyclic, then $(r, \mathcal{G})$ is also a sync-pair. Therefore, there is no gap between the sufficiency results of Theorems 1 and 2.

Toward the end of this section, we present a result that combines Proposition 1 and Theorem 1. Recall that a rooted digraph $\mathcal{G}$ is said to be quasi-acyclic if all the cycles of $\mathcal{G}$ are in its root component $\mathcal{G}_R = (\mathcal{V}_R, \mathcal{E}_R)$. The digraph $\mathcal{G}_c$ obtained by condensing the root component to a single vertex is rooted acyclic (see Fig. 4 for illustration). We show that robust fixed-time synchronization can be achieved for these digraphs as well. The trade-off is that the partition vector is not free to choose anymore, and there is an upper bound for every r_i, with $i \in \mathcal{V}_R$, of order $\mathcal{O}(\frac{1}{|\mathcal{V}_R|})$. Since the proof follows similar steps as the proof of Theorem 1, we present the result as a corollary.

Corollary 1. *Let $\mathcal{G}$ be rooted and quasi-acyclic, with $\mathcal{V}_R$ the root set. If $r_i \in (0, \frac{1}{|\mathcal{V}_R|-1})$ for any $i \in \mathcal{V}_R$, then $(r, \mathcal{G})$ is a sync-pair. Moreover, (28) holds for $T^* = (\mathrm{dep}(\mathcal{G}_c) + 2)T$.*

Proof. By Proposition 1, the agents in the root component will reach synchronization in no more than $2T$ seconds and stay synchronized after that. We can thus treat all the roots as a whole. After condensing the root component to a single vertex, the resulting digraph $\mathcal{G}_c$ is rooted acyclic. Theorem 1 then applies to the case, which completes the proof. ■

Since any strongly connected digraph $\mathcal{G}$ satisfies $\mathrm{dep}(\mathcal{G}_c) = 0$, and any rooted acyclic digraph satisfies $\mathrm{dep}(\mathcal{G}_c) = \mathrm{dep}(\mathcal{G})$, the bound T^* on the convergence time t established in Corollary 1 generalizes the bounds obtained in Proposition 1 and Theorem 1. However, as mentioned before, this generality comes at the price of the scalability of the partition vector r. The entries of r are of order $\mathcal{O}(\frac{1}{|\mathcal{V}_R|})$, which tend to 0 as $|\mathcal{V}_R| \to \infty$. Nevertheless, as we will show in the next section, the scalability property of r can be fully recovered by adding suitable randomness into the PCOs.

Remark 7. Given that Theorems 1–2, and Corollary 1 guarantee fixed-time synchronization of the PCOs, it is clear that all our results also hold if the digraph $\mathcal{G}_t$ is time-varying and (T^*, L)-*persistently rooted acyclic* (Poveda & Teel, 2019a, Def. 3), i.e., if for each interval I of length L there exists a sub-interval $I_i = [t_i, t_{i+1}] \subset I$ satisfying $t_{i+1} - t_i = T^*$ and a rooted acyclic digraph $\mathcal{G}^*$ such that $\mathcal{G}_t = \mathcal{G}^*$ for all $t \in I_i$.

4. Stochastic resetting algorithms

In this section, we consider networks of PCOs implementing the same hybrid update rule (1), (2), and (7), but with the underlying communication network being a random digraph. In this setting, every time an agent resets its phase to 1, it generates *i.i.d.* Bernoulli random variables to decide whether or not to send pulses to its out-neighbors. In order to formalize the model of the system, we will use the framework of set-valued stochastic hybrid dynamical systems (SHDS) (Subbaraman & Teel, 2016; Teel, Subbaraman, & Sferlazza, 2014).

4.1. Well-posed stochastic hybrid model

To formalize the model of the PCOs with random digraphs, we start by fixing a deterministic digraph $\mathcal{G} := (\mathcal{V}, \mathcal{E})$. Let $\mathcal{G}' = (\mathcal{V}, \mathcal{E}')$ be a subgraph of $\mathcal{G}$, with the same vertex set $\mathcal{V}$ and $\mathcal{E}' \subseteq \mathcal{E}$. We call any such digraph $\mathcal{G}'$ a ***feasible*** digraph. Note that every feasible digraph $\mathcal{G}'$ can be represented by a binary vector $v \in \{0,1\}^{|\mathcal{E}|}$ as follows:

$$v := [\ldots, v_{ij}, \ldots], \tag{29}$$

where each entry v_{ij} indicates whether $(i,j) \in \mathcal{E}$ is an edge of $\mathcal{G}'$ or not: If $v_{ij} = 1$, then $(i,j) \in \mathcal{E}'$. Otherwise, $(i,j) \notin \mathcal{E}'$. Note that the binary vectors in $\{0,1\}^{|\mathcal{E}|}$ one-to-one correspond to the feasible digraphs. For convenience, we will let $\Psi := \{0,1\}^{|\mathcal{E}|}$, be the set of all feasible digraphs represented by the binary vectors v.

We next consider an Erdös–Rényi type random graph model for generating a feasible digraph. For a given vector $v \in \Psi$, we let the entries v_{ij} be *i.i.d.* Bernoulli (p) random variables, i.e., the probability that v_{ij} takes value 1 (resp. 0) is p (resp. $(1-p)$). We denote by μ the probability measure for the random graph. It follows that for any feasible digraph $\mathcal{G}' = (\mathcal{V}, \mathcal{E}')$,

$$\mu(\mathcal{G}') = p^{|\mathcal{E}'|}(1-p)^{|\mathcal{E}|-|\mathcal{E}'|}. \tag{30}$$

We will now adapt the resetting algorithm to accommodate the above random graph model. First, note that the communication digraph affects (only) the jump map of the hybrid dynamics (8). In the previous deterministic setting, the digraph is always given by $\mathcal{G}$. For the stochastic setting, we replace $\mathcal{G}$ with a random graph $\mathcal{G}'$, with $\mathcal{G}' \sim \mu(\cdot)$. Furthermore, if we let $\mathcal{G}_k$, for $k \in \mathbb{N}$, be the feasible digraph at discrete time k (i.e., the communication digraph at the occurrence of the kth jump), then all these digraphs are independent of each other. In other words, the sequence $\{\mathcal{G}_k\}_{k=1}^{\infty}$ comprises *i.i.d.* random variables, with $\mathcal{G}_k \sim \mu(\cdot)$.

We note here that a similar random graph model has been considered in Klinglmayr et al. (2017, 2012). The key difference is that the model of Klinglmayr et al. (2017, 2012) considered the

following scenario: Whenever an agent jumps, it draws *only one* Bernoulli random variable to decide whether it sends pulses to *all* of its out-neighbors or not. However, the digraphs considered in these two papers were either bi-directional or strongly connected. Whether their random graph model can work for rooted graphs is a non-trivial question, which we will address on another occasion. Another major difference from the works in Klinglmayr et al. (2017, 2012) is that we utilize tools from stochastic hybrid dynamical system to analyze the well-posedness, stability, and convergence properties of the PCOs. Indeed, given that standard PCOs are hybrid dynamical systems, the addition of randomness into the model naturally leads to a stochastic hybrid setting.

To construct the corresponding SHDS, it suffices to re-define the jump map. It takes three steps to do so. First, for each edge $(i,j) \in \mathcal{E}$, we consider the set-valued mapping $S_{ij} : [0,1] \times \Psi \rightrightarrows [0,1]$ as follows:

$$S_{ij}(\tau_j, v) = v_{ij}\overline{\mathcal{P}}(\tau_j) + (1 - v_{ij})\tau_j, \tag{31}$$

where $\overline{\mathcal{P}}$ is the BPR given by (7), and v_{ij} is the entry that corresponds to the edge (i,j) in $\mathcal{E}$. Next, using (31), we define a new set-valued mapping $G_v^0 : [0,1]^N \times \Psi \rightrightarrows \mathbb{R}^N$ as follows:

$$G_v^0(\tau, v) := \Bigg\{ g \in \mathbb{R}^N : g_i = 0, \quad g_j \in \left\{ \begin{array}{ll} S_{ij}(\tau_j, v), & (i,j) \in \mathcal{E} \\ \{\tau_j\}, & (i,j) \notin \mathcal{E} \end{array} \right\}, \ \forall\, j \neq i \Bigg\}, \tag{32}$$

which is defined to be nonempty only when $\tau_i = 1$ for some $i \in \mathcal{V}$ and $\tau_j \in [0,1)$ for $j \neq i$. Finally, the jump map for the SHDS is defined as the outer-semicontinuous hull of G_v^0, i.e.,

$$G_v(\tau, v) := \overline{G_v^0(\tau, v)}. \tag{33}$$

Note that when a jump occurs and a random graph $\mathcal{G}_k$ is drawn, not every edge of $\mathcal{G}_k$ plays a role in the jump map G_v. Only the edges (i,j) with $\tau_i = 1$ for some $i \in \mathcal{V}$, matter. Thus, an agent i does not need to know the structure of the entire graph $\mathcal{G}_k$, but rather its out-neighbors (as the set of agents it needs to send pulses from time to time). Correspondingly, the out-going edges of the agent i are completely determined by the agent through the *i.i.d.* Bernoulli random variables that are generated locally by agent i itself. The reason of including the entire graph $\mathcal{G}_k$ in the jump map G_v is rather for ease of analysis.

The following lemma establishes that the jump map G_v satisfies the Basic Conditions of Definition 1.

Lemma 5. *The set-valued mapping $G_v : [0,1]^N \times \Omega \rightrightarrows [0,1]^N$ defined by (33) satisfies condition (c) of Definition 1.*

Proof. We start by considering the set-valued map S_{ij} of (31). For each fixed τ, the mapping S_{ij} is a summation of two measurable maps. Thus, by Rockafellar and Roger (1998, Prop. 14.11), the mapping S is measurable with respect to v. Since for each $\tau \in \mathbb{R}^N$ the mapping $G^0(\tau, v)$ in (32) is constructed by assigning 0 to the ith component, and $S_{ij}(\tau_j, v)$ or τ_j to the other components, it follows that $v \mapsto G^0(\tau, v)$ is also measurable. Finally, measurability of the mapping $v \mapsto \text{graph}(G(\cdot, v))$ follows from the fact that G is outer semicontinuous (Teel, 2013, Appendix A.2.). Since by construction G is locally bounded, it follows that it satisfies the basic conditions. ■

Note that the digraph $\mathcal{G}$ and the probability $p \in [0,1]$ of the Bernoulli distribution uniquely determine the probability space $(\Omega, \mathcal{F}, \mu)$. Thus, the resulting SHDS depends on three parameters, namely, p, r, and $\mathcal{G}$.

We will write the SHDS as

$$\mathcal{H}_S(p, r, \mathcal{G}) := (C, f, D, G_v), \tag{34}$$

where the subindex S indicates that the system is stochastic.

Remark 8. An important standing assumption of our model, embedded in the definition of random solutions used in the paper, is the *causal* dependence of the solutions on the random variables. In particular, note that the condition $\tau_i = r_i$, or the existence of more than one agent satisfying the condition $\tau_i = 1$, leads to a set $G_v(\tau, v)$ in (33) that has more than one element. In this case, our model will require that each particular selection $\tau^+ \in G_v(\tau, v)$ should not be able to anticipate the next communication graph $\mathcal{G}_k$ that will be assigned to the agents at the next jump. This causality property is specified in Appendix C. As shown in Teel (2013), the causality property is needed in order to make use of suitable Lyapunov-based arguments for the stability analysis of the system via invariance-like principles. Causality is a standard assumption in stochastic algorithms.

As highlighted in Remarks 2 and 8, it is important to note that in our model for each fixed $\omega \in \Omega$ the sample path τ_ω generated by the SHDS (34) may not be unique, and the analysis of each individual solution becomes intractable as N increases. This feature makes the stability analysis of the set-valued stochastic synchronization dynamics non-trivial and differs from previous results in the literature that relied on single-valued update rules (Klinglmayr et al., 2017, 2012).

4.2. Almost sure global synchronization: Stability and attractivity

We recall that the compact set $\mathcal{A}_s$ is defined in (14), which captures all synchronized states of the network. Similar to the definition of sync-pairs for deterministic HDS, we introduce the following definition for SHDS:

Definition 5. Let $\mathcal{A}_s$ be given in (14). Let $p \in [0,1]$, $r \in [0,1)^N$, and $\mathcal{G}$ be a digraph of N vertices. Then, $(p, r, \mathcal{G})$ is a **sync-triplet** if

(a) For every initial condition in $C \cup D$, there exist non-trivial solutions of $\mathcal{H}_S(p, r, \mathcal{G})$ almost surely (see Appendix B for the definition), and every maximal solution is complete and uniformly Non-Zeno almost surely;
(b) The SHDS $\mathcal{H}_S(p, r, \mathcal{G})$ renders $\mathcal{A}_s$ UGASp.

Note that a *necessary* condition for $(p, r, \mathcal{G})$ to be a sync-triplet is that $\mathcal{G}$ is rooted. This fact can be established by using the same arguments as in the proof of Proposition 2. However, in contrast to the deterministic setting (cf. Proposition 3), we will see soon that having a rooted digraph $\mathcal{G}$ is also a *sufficient* condition for $(p, r, \mathcal{G})$ to be a sync-triplet.

For ease of presentation, we let $\omega := \omega_1\omega_2\omega_3\cdots$ be a sequence of *i.i.d.* random variables, with each $\omega_i \sim \mu(\cdot)$ a feasible digraph. We denote by Ω the collection of sample paths ω. It should be clear that for an event:

$$\Omega' := \{\omega \in \Omega \mid \omega_1 = v_1, \ldots, \omega_k = v_k\}$$

with $v_i \in \Psi$ for all $i = 1, \ldots, k$, its probability is given by $\mathbb{P}(\Omega') = \prod_{i=1}^k \mu(v_i)$. Note that a sample path ω determines the underlying digraphs for jumps at all discrete times k, for $k \geq 1$. A solution of $\mathcal{H}_S(p, r, \mathcal{G})$ thus depends on ω and we denote it by $\boldsymbol{\tau}_\omega$. Note that there may exist multiple solutions even if we fix ω and the initial condition, which is due to the set-valued nature of the jump map in the SHDS. For each solution we further define the following random variable:

$$\boldsymbol{T}^*(\boldsymbol{\tau}_\omega) := \inf\{t \mid \boldsymbol{\tau}_\omega(t,j) \in \mathcal{A}_s,\ (t,j) \in \text{dom}(\boldsymbol{\tau}_\omega)\}, \tag{35}$$

which is the first hitting-time for the solution $\boldsymbol{\tau}_\omega$ to enter the compact set $\mathcal{A}_s$ (i.e., the instant at which the SHDS achieves synchronization for the first time). We establish below the following result:

Theorem 3. *If $p \in (0,1)$, $r \in (0,1)^N$, and $\mathcal{G}$ is a rooted directed graph, then $(p, r, \mathcal{G})$ is a sync-triplet. Moreover, for any initial condition $\tau_\omega(0,0)$, the following holds for all positive integers n and all random solutions $\boldsymbol{\tau}_\omega$ of the SHDS:*

$$\mathbb{P}\left(\boldsymbol{T}^*(\boldsymbol{\tau}_\omega) > nT^*\right) \leq \rho^n, \tag{36}$$

where T^* is given in (28) and $\rho \in (0,1)$ is the constant:

$$\rho := 1 - \left(p^{N-1}(1-p)^{|\mathcal{E}|-N+1}\right)^{\text{dep}(\mathcal{G})\ell^*}, \tag{37}$$

where $\ell^* = N(\lfloor 1/\underline{r} \rfloor + 1)$, with $\underline{r} = \min_{i\in\mathcal{V}} r_i$, as introduced in Lemma 2,

Remark 9. Note that by Theorem 3, the stochastic resetting algorithm is scalable because neither p nor r_i, for $i \in \mathcal{V}$, depends on the size N of the network. We also note that the result can be further generalized by allowing different agents to have heterogeneous probabilities $p_{ij} \in (0,1)$, for $(i,j) \in \mathcal{E}$, as the parameters of the Bernoulli random variables. Correspondingly, the expression (37) will be changed as follows: first, let $\underline{p} := \min\{p_{ij} \mid (i,j) \in \mathcal{E}\}$ and $\bar{p} := \max\{p_{ij} \mid (i,j) \in \mathcal{E}\}$; then, replace in (37) the term p^{N-1} with $\underline{p}^{N-1}$ and the term $(1-p)^{|\mathcal{E}|-N+1}$ with $(1-\bar{p})^{|\mathcal{E}|-N+1}$. With slight modification, the analysis we carry out below can still apply to establish the proof for the heterogeneous case. However, for clarity of presentation, we will focus only on the homogeneous case where p is the same for all agents.

Below, we present the proof of Theorem 3. To proceed, we first establish some preliminary lemmas. We define $\mathcal{S}(\tau_0)$ as the set of all maximal random solutions of (34) from the initial condition $\tau_\omega(0,0) = \tau_0 \in C \cup D$. For each feasible initial condition, we define the following event:

$$\begin{aligned}\Omega_1(\tau_\omega(0,0)) := \Big\{ & \omega \in \Omega \mid \forall\ \tau_\omega \in \mathcal{S}(\tau_\omega(0,0)), \exists\ i^* \in \mathcal{V}_R \\ & \text{and } \exists\ (t^*_\omega, j^*_\omega) \in \text{dom}(\tau_\omega) \text{ with } t^*_\omega \leq T \\ & \text{s.t. } \tau_{\omega,i^*}(t^*_\omega, j^*_\omega) = 1 \Big\}.\end{aligned} \tag{38}$$

Lemma 6. *For any $\tau_\omega(0,0) \in C \cup D$, $\Omega_1(\tau_\omega(0,0)) = \Omega$.*

Proof. The result follows directly from the fact that a root can only be influenced by another root and by the fact that τ always increases during flows. ■

Next, we recall a fact from graph theory:

Lemma 7. *For a rooted digraph $\mathcal{G}$ with a root i^*, there exists a directed spanning tree $\mathcal{T}_{i^*}$ with i^* the unique root.*

Proof. One can generate a desired $\mathcal{T}_{i^*}$ using the breadth-first search algorithm (Graham, Grötschel, & Lovász, 1995). ■

Note that for a given root i^* of $\mathcal{G}$, there may exist multiple directed spanning trees with i^* the root. In the sequel, we will fix $\mathcal{T}_{i^*}$ for each root i^* so that the map $i^* \mapsto \mathcal{T}_{i^*}$ is well defined.

Next, we let l and L be two positive integers. Then, for the given l and L and for a given root i^* of $\mathcal{G}$, we define another event as follows:

$$\Omega_2(l, L, i^*) := \{\omega \in \Omega \mid \omega_k = \mathcal{T}_{i^*},\ \forall k = l+1, \ldots, l+L\}. \tag{39}$$

In words, the above event is defined such that the random digraphs ω_k, for $k = l+1, \ldots, l+L$, are the same and given by a certain directed spanning tree with root i^*. We introduce such an event so as to make a connection with Theorem 1, details of which will be elaborated soon in the proof of Theorem 3.

We have the following fact:

Lemma 8. *For any given positive integers l and L and for any root i^* of $\mathcal{G}$,*

$$\mathbb{P}(\Omega_2(l, L, i^*)) = \left(p^{N-1}(1-p)^{|\mathcal{E}|-N+1}\right)^L. \tag{40}$$

Proof. The result follows from the fact that the random variables ω_k, for $k \geq 1$, are *i.i.d.* and, moreover, $\mu(\mathcal{T}_{i^*}) = p^{N-1}(1-p)^{|\mathcal{E}|-N+1}$ where the integer $(N-1)$ is the number of edges of a directed spanning tree with N vertices. ■

With the above lemmas, we are now in a position to prove Theorem 3:

Proof of Theorem 3. We first establish the fact that $(p, r, \mathcal{G})$ is a sync-triplet. Consider again the Lyapunov function $V : [0,1]^N \to \mathbb{R}_{\geq 0}$ defined as the infimum of all arcs that touch all agents on the unit circle, where the points 0 and 1 are identified to be the same. This function is positive definite with respect to the set $\mathcal{A}_s$, it is uniformly bounded as $V(\boldsymbol{\tau}_\omega) \leq 1 - \frac{1}{N}$ for all $\boldsymbol{\tau}_\omega \in [0,1]^N$, and it does not increase during flows of the SHDS (34) surely, i.e, $\dot{V}(\boldsymbol{\tau}_\omega) \leq 0$ for all $\boldsymbol{\tau}_\omega \in C$. By construction of V, since the number of points occupied by agents in the circle cannot increase, we also have that V does not increase during jumps. Moreover, by construction of the sets C and D, the continuity of the mapping f in (10), and Lemma 5, the SHDS satisfies the basic conditions. Also, by using the same arguments of the proof of Lemma 2, it follows that every solution of the SHDS is surely complete. Thus, by the stochastic hybrid invariance principle (c.f. Theorem C.1 in Appendix C) in order to show UGASp of the set $\mathcal{A}_s$, it suffices to show that there does not exist almost surely complete solutions $\boldsymbol{\tau}_\omega$ that remain in a non-zero level set of the Lyapunov function almost surely.

To establish the above fact, we will show that there exist positive constants α and T^* such that for any initial condition $\tau_\omega(0,0) \in [0,1]^N$, the following holds:

$$\mathbb{P}(\Omega_3(\tau_\omega(0,0))) > \alpha, \tag{41}$$

where the event $\Omega_3(\tau_\omega(0,0))$ is given by

$$\begin{aligned}\Omega_3(\tau_\omega(0,0)) := \Big\{ & \omega \in \Omega \mid \forall\ \boldsymbol{\tau}_\omega \in \mathcal{S}(\tau_\omega(0,0)) \text{ and } \forall\ t \geq T^* \\ & \text{s.t. } (t,j) \in \text{dom}(\tau_\omega),\ V(\boldsymbol{\tau}_\omega(t,j)) = 0 \Big\}.\end{aligned}$$

We show below that α and T^* can be chosen to be the following values $\alpha := 1 - \rho$, where $\rho \in (0,1)$ is defined in (37), and $T^* := (\text{dep}(\mathcal{G}) + 1)T$.

First, by Lemma 6, for any solution $\boldsymbol{\tau}_\omega$, there exist a hybrid time (t^*_ω, j^*_ω), with $t^*_\omega \leq T$, and a root i^* of $\mathcal{G}$ such that $\boldsymbol{\tau}_{\omega,i^*}(t^*_\omega, j^*) = 1$. Conditioning on the fact that $\boldsymbol{\tau}_{\omega,i^*}(t^*_\omega, j^*_\omega) = 1$, we consider the event $\Omega_2(j^*_\omega, j^*_\omega + L, \mathcal{T}_{i^*})$, where $L := \text{dep}(\mathcal{T}_{i^*})\ell^*$, and $\ell^* = N(\lfloor 1/\underline{r} \rfloor + 1)$ with $\underline{r} = \min_{i\in\mathcal{V}} r_i$. Note that by Lemma 2, for the discrete time j to increase from j^*_ω to $j^*_\omega + L$, the continuous time has to increase at least $\text{dep}(\mathcal{T}_{i^*})T$ because otherwise, there will not be as many as L jumps. For convenience, we let t^{**}_ω be the time that the $(j^* + L)$th jump occurs. By definition of the event $\Omega_2(j^*, L, i^*)$ (see (39)), the underlying digraph during this period $[t^*_\omega, t^{**}_\omega]$ is given by the directed spanning tree $\mathcal{T}_{i^*}$. Thus, following the same arguments used in the proof of Theorem 1, we have that the solution $\boldsymbol{\tau}_\omega$ will reach synchronization at time $t^*_\omega + \text{dep}(\mathcal{T}_{i^*})T \leq t^{**}_\omega$. Further, since $\text{dep}(\mathcal{T}_{i^*}) \leq \text{dep}(\mathcal{G})$ and since $t^*_\omega \leq T$ (by Lemma 6), we have that $t^*_\omega + \text{dep}(\mathcal{T}_{i^*})T \leq T^*$. The above arguments imply that $V(\boldsymbol{\tau}_\omega(t,j)) = 0$, for all $t \geq T^*$. Thus,

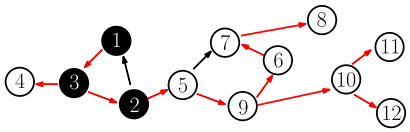

Fig. 5. Rooted digraph with vertices 1, 2, and 3 being roots. The connections in red indicate a directed spanning tree with maximum depth.

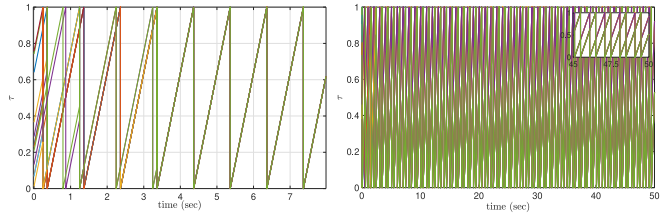

Fig. 6. Solutions generated by the HDS (8) for the network topology given in Fig. 5. Left: Synchronization is achieved in approximately 3.4 s when each agent picks $r_i \in (0, \frac{1}{2})$. Right: Synchronization is not achieved when r_2 is set to be 3/4.

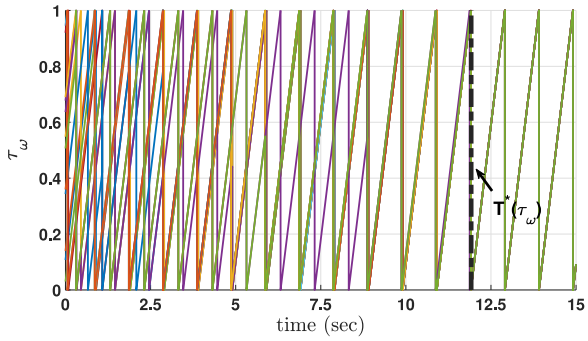

Fig. 7. A sample path generated by the SHDS (34) for the network topology given in Fig. 5. Synchronization is achieved in approximately 12 s for this sample path.

to establish (41), it now remains to show that the probability of the event $\Omega_2(j^*, L, i^*)$ is a nonzero constant, but this is given by Lemma 8 with $\mathbb{P}(\Omega_2(j^*, L, i^*)) = \alpha$.

Finally, we show that (36) holds. The computation in fact follows from the above argument. First, by the Bayes rule, we have that

$$\mathbb{P}\left(\boldsymbol{T}^*(\boldsymbol{\tau}_\omega) > nT^*\right) = \mathbb{P}\left(\boldsymbol{T}^*(\boldsymbol{\tau}_\omega) > (n-1)T^*\right) \cdots \\ \cdots \times \mathbb{P}\left(\boldsymbol{T}^*(\boldsymbol{\tau}_\omega) > nT^* \,|\, \boldsymbol{T}^*(\boldsymbol{\tau}_\omega) > (n-1)T^*\right).$$

Using the Markovian property, the conditional probability on the right hand side of the above expression can be written as $\mathbb{P}(\boldsymbol{T}^*(\boldsymbol{\tau}'_{\omega'}) > T^*)$, where $\boldsymbol{\tau}'_{\omega'}$ is a new solution with the initial condition $\tau'_{\omega'}(0,0)$ given by $\tau'_{\omega'}(0,0) = \tau_\omega((n-1)T^*, j)$, for some j and $\omega' := \omega_{j+1}\omega_{j+2}\cdots$. Note that by definition of $\Omega_3(\tau'_{\omega'}(0,0))$ and (41), we have that

$$\mathbb{P}\left(\boldsymbol{T}^*(\boldsymbol{\tau}'_{\omega'}) > T^*\right) = 1 - \mathbb{P}(\Omega_3(\tau'_{\omega'}(0,0))) < 1 - \alpha = \rho.$$

It then follows that

$$\mathbb{P}\left(\boldsymbol{T}^*(\boldsymbol{\tau}_\omega) \geq nT^*\right) < \rho\mathbb{P}\left(\boldsymbol{T}^*(\boldsymbol{\tau}_\omega) \geq (n-1)T^*\right).$$

The above recursive formula then implies that (36) holds. ■

5. Numerical studies

In this section, we illustrate our theoretical results via numerical examples. We consider a network of $N = 12$ PCOs.

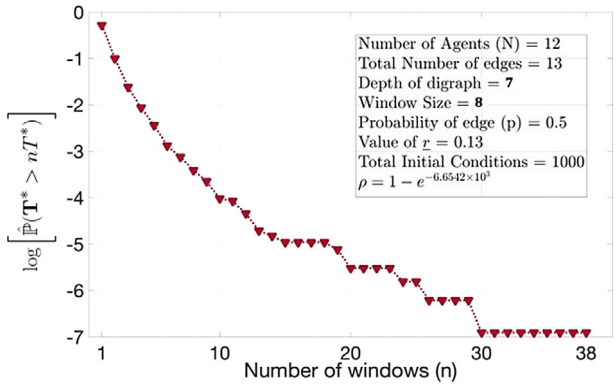

Fig. 8. This figure plots $\log(\hat{\mathbb{P}}(\mathbf{T}^* > nT^*))$ versus the number n of windows needed for a sample path to achieve synchronization. There are 1000 sample paths simulated.

The underlying digraph is rooted as shown in Fig. 5. A directed spanning tree with maximum depth is indicated by red arrows. The depth of the tree is 7. We set the period of the PCOs as $T = 1$, which implies that the constant $T^* = (\text{dep}(\mathcal{G}) + 1)T$ introduced in (28) is equal to 8. We also note that $(\text{dep}(\mathcal{G}_c) + 2)T = 7$ where $\mathcal{G}_c$ is the condensed digraph of $\mathcal{G}$. We first simulate the HDS (8) over the digraph $\mathcal{G}$. First, we let each agent sample its r_i uniformly randomly from $(0, \frac{1}{2})$. By doing so, the condition of Corollary 1 is satisfied. We next let agents sample their initial conditions uniformly randomly from $(0, 1)$. On the left of Fig. 6, we present a sample trajectory for one of such initial conditions. The entire network achieves synchronization in 3.4 s (within 7 s) which agrees with the statement of Corollary 1. However, if we change the parameter r_2 of agent 2 to be $\frac{3}{4}$ (which is greater than $\frac{1}{2}$) and keep the other r_i's unchanged. Then, the network is not guaranteed to reach synchronization anymore. On the right of Fig. 6, we present a sample trajectory that does not reach synchronization (over a long time interval).

We now simulate the SHDS (34) over the same digraph $\mathcal{G}$ as above. This time, we let the parameters r_i be uniformly randomly chosen out of $(0, 1)$. The probability p of drawing an out-going edge is 0.5. In Fig. 7, we show a sample path generated by the SHDS (34). Then, we investigate the first hitting time $\boldsymbol{T}^*(\boldsymbol{\tau}_\omega)$ defined in (35) using the same SHDS. We choose 1000 random initial conditions uniformly from $(0, 1)^N$. For each initial condition, we let $((n-1)T^*, nT^*]$, for $n \geq 1$, be the window that contains $\boldsymbol{T}^*(\boldsymbol{\tau}_\omega)$ (i.e., the sample path reaches synchronization during that period). In Fig. 8, we plot the empirical version of $\mathbb{P}(\mathbf{T}^* > nT^*)$ for different n, i.e., we plot $\hat{\mathbb{P}}(\mathbf{T}^* > nT^*) := 1 - \sum_{k=1}^{n} \frac{\text{Freq}(k)}{1000}$, where Freq$(k)$ is the total number of times that the first hitting time $\mathbf{T}^*(\boldsymbol{\tau}_\omega)$ belongs to $((n-1)T^*, nT^*]$. The plot is in the log scale.

Furthermore, we investigate the dependence of the first hitting time $\boldsymbol{T}^*(\boldsymbol{\tau}_\omega)$ on the size N of network. We simulate the SHDS on three different classes of network topologies: complete digraphs, cycle digraphs, and path digraphs. For each class, we vary the number N of agents from 10 to 250, with increments of 10. The parameters r_i are again chosen uniformly randomly from $(0, 1)$ and the probability p of drawing an edge is 0.5. For each case (with a fixed class and a fixed size N), we generate 100 initial conditions uniformly randomly from $(0, 1)^N$ and simulate the SHDS (34). For each sample path, we record the first hitting time $\boldsymbol{T}^*(\boldsymbol{\tau}_\omega)$. Figs. 9, 10, and 11 plot the data for complete-, cycle-, and path-digraphs, respectively. For each figure, the horizontal axis is the network size N and the vertical axis is the first hitting time $\boldsymbol{T}^*(\boldsymbol{\tau}_\omega)$. For each N, the crosses represent the first hitting times of the sample paths. There are 100 of them and the red

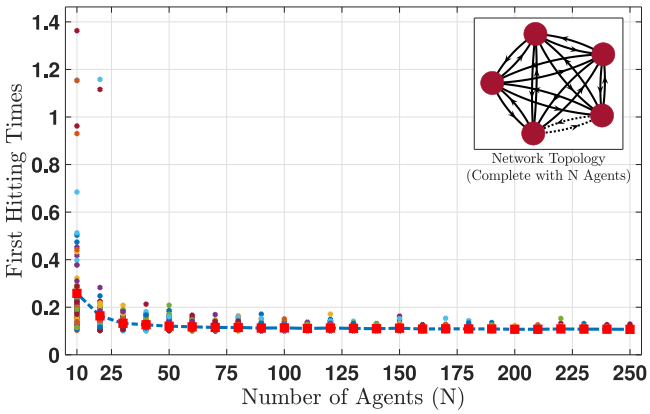

Fig. 9. First hitting time vs size of complete digraph. (For interpretation of the references to color in this figure legend, the reader is referred to the web version of this article.)

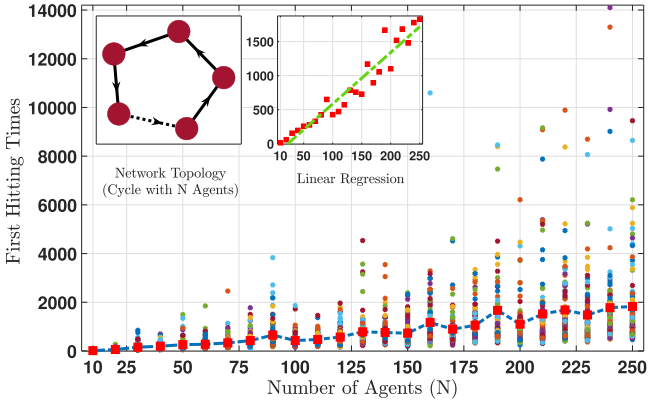

Fig. 10. First hitting time vs size of cycle digraph. (For interpretation of the references to color in this figure legend, the reader is referred to the web version of this article.)

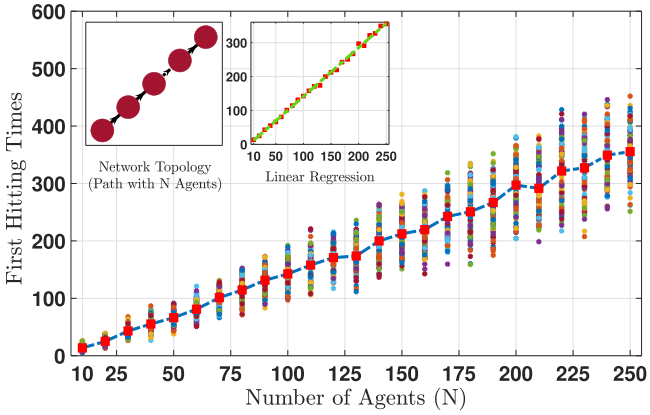

Fig. 11. First hitting time vs size of path digraph. (For interpretation of the references to color in this figure legend, the reader is referred to the web version of this article.)

square is the mean. For complete digraphs, the mean decays to a steady state. The variance seems to decay as well. However, this is not the case for cycles or paths. In either case, the average and the variance increase as N grows. Using linear regression, we find that the fitting curves for paths and cycles are $1.4N - 2.6$ and $7.5N - 170.6$, respectively.

6. Conclusions

In this paper we have established several new results about synchronization of pulse-coupled oscillators over directed graphs, amongst which there are two major ones: We have shown that robust global fixed-time synchronization can be achieved over quasi-acyclic digraphs using a deterministic binary resetting algorithm, where turning parameters are independent of network sizes. Further, by accommodating an Erdös–Renýi type random graph model, we have developed a scalable stochastic binary resetting algorithm by which global synchronization can be achieved, with probability one, over rooted digraphs. Future directions will study the development of similar stochastic coordination algorithms for multi-time scale hybrid dynamical systems.

Appendix A. Notation and definitions

A set-valued mapping $M : \mathbb{R}^m \rightrightarrows \mathbb{R}^n$ is said to be outer semi-continuous (OSC) at $x \in \mathbb{R}^m$ if for all sequences $x_i \to x$ and $y_i \in M(x_i)$ such that $y_i \to y$ we have that $y \in M(x)$. A set-valued mapping $M : \mathbb{R}^m \rightrightarrows \mathbb{R}^n$ is said to be locally bounded (LB) at $x \in \mathbb{R}^m$ if there exists a neighborhood K_x of x such that $M(K_x)$ is bounded. Given a set $\mathcal{X} \subset \mathbb{R}^m$, the mapping M is OSC and LB relative to $\mathcal{X}$ if the set-valued mapping from $\mathbb{R}^m$ to $\mathbb{R}^n$ defined by M for $x \in \mathcal{X}$, and by $\varnothing$ for $x \notin \mathcal{X}$, is OSC and LB at each $x \in \mathcal{X}$. The graph of a set-valued mapping G is defined as $\text{graph}(G) := \{(x, y) \in \mathbb{R}^m \times \mathbb{R}^n : y \in G(x)\}$. Given a set $B \subset \mathbb{R}^n$, we use $\text{cl}(B)$ to denote its closure. The outer semi-continuous hull of G is the unique set-valued mapping $\overline{G} : \mathbb{R}^m \rightrightarrows \mathbb{R}^n$ satisfying $\text{graph}(\overline{G}) = \text{cl}(\text{graph}(G))$, (Rockafellar & Roger, 1998, pp. 155). Given a measurable space $(\Omega, \mathcal{F})$, a set-valued map $G : \Omega \rightrightarrows \mathbb{R}^n$ is said to be $\mathcal{F}$-*measurable* (Rockafellar & Roger, 1998, Def. 14.1), if for each open set $\mathcal{O} \subset \mathbb{R}^n$, the set $G^{-1}(\mathcal{O}) := \{\omega \in \Omega : G(\omega) \cap \mathcal{O} = \varnothing\} \in \mathcal{F}$. A sequence of maps $x_i : \text{dom}(x_i) \to \mathbb{R}^n$ is said to converge graphically if the sequence of sets $\{\text{graph}(x_i)\}_{i=1}^{\infty}$ converges in the sense of set convergence (Goebel et al., 2012, Def. 5.1).

Appendix B. Hybrid dynamical systems

A HDS is characterized by the following inclusions (Goebel et al., 2012):

$$x \in C, \qquad \dot{x} = f(x), \tag{B.1a}$$

$$x \in D, \qquad x^+ \in G(x), \tag{B.1b}$$

where $x \in \mathbb{R}^n$ is the state of the system, $f : \mathbb{R}^n \to \mathbb{R}^n$ is the flow map, which describes the continuous-time dynamics of the state; $C \subset \mathbb{R}^n$ is called the flow set and it describes the points in the space where x is allowed to evolve according to the differential equation (B.1a); $G : \mathbb{R}^n \times \mathbb{R}^m \rightrightarrows \mathbb{R}^n$ is the jump map and it characterizes the discrete-time dynamics of x; and $D \subset \mathbb{R}^n$ is called the jump set and it describes the points in the space where x is allowed to evolve according to the set-valued update (B.1b). The HDS is represented as $\mathcal{H} = \{C, D, F, G\}$. In this paper we restrict our attention to HDS that satisfy the basic conditions of Definition 1. A standard solution x to (B.1) is parameterized by a continuous-time index t and a discrete-time index j. In particular, solutions to (B.1) are defined on hybrid time domains. A compact hybrid time domain is a subset of $\mathbb{R}_{\geq 0} \times \mathbb{Z}_{\geq 0}$ of the form $\cup_{j=0}^{J}([t_j, t_{j+1}] \times \{j\})$ for some $J \in \mathbb{Z}_{\geq 0}$ and real numbers $0 = t_0 \leq t_1 \leq \cdots \leq t_{J+1}$. A hybrid time domain is a set $E \subset \mathbb{R}_{\geq 0} \times \mathbb{Z}_{\geq 0}$ such that for each T, J, the set $E \cap ([0, T] \times \{0, 1, 2, \ldots, J\})$ is a compact hybrid time domain. A function $x : E \to \mathbb{R}^n$ is said to be a hybrid arc if E is a hybrid time domain, and for each j such that the interval $I_j = \{t \geq 0 : (t, j) \in \text{dom}(x)\}$ has non-empty interior the function $t \mapsto x(t, j)$ is locally absolutely continuous. A hybrid

arc x is said to be a solution to a HDS (B.1) satisfying the basic conditions if: (1) $x(0,0) \in C \cup D$. (2) If $(t_1,j),(t_2,j) \in \text{dom}(x)$ with $t_1 < t_2$, then for almost every $t \in [t_1,t_2]$, $x(t,j) \in C$ and $\dot{x}(t,j) = f(x(t,j))$. (3) If $(t,j),(t,j+1) \in \text{dom}(x)$, then $x(t,j) \in D$ and $x(t,j+1) \in G(x(t,j))$. A solution x to (B.1) is said to be: (a) *non-trivial* if $\text{dom}(x)$ contains at least two points; (b) *maximal* if there does not exist another solution x' to $\mathcal{H}$ such that $\text{dom}(x) \subsetneq \text{dom}(x')$ and $x(t,j) = x'(t,j)$ for all $(t,j) \in \text{dom}(x)$; (c) *complete* if its domain is unbounded; (d) *eventually discrete* if $T = sup_t \text{dom}(x) < \infty$ and $\text{dom}(x) \cap (\{T\} \times \mathbb{N})$ contains at least two points. d) *uniformly non-Zeno* if there exists $(T,J) \in \mathbb{R}_{>0}$ such that for every $(t_1,j_1),(t_2,j_2) \in \text{dom}(x)$, if $t_2 - t_1 \leq T$ then $j_2 - j_1 \leq J$.

Appendix C. Stochastic hybrid dynamical systems

When the jump map in (B.1b) also depends on a random input $\mathbf{v}$, the HDS (B.1) becomes a SHDS (Subbaraman & Teel, 2016) of the form

$$x \in C, \qquad \dot{x} = f(x), \tag{C.1a}$$

$$x \in D, \qquad x^+ \in G(x, v^+), \quad v \sim \mu(\cdot), \tag{C.1b}$$

where v^+ is a place holder for a sequence $\{\mathbf{v}_k\}_{k=1}^{\infty}$ of independent, identically distributed *i.i.d.* input random variables $\mathbf{v}_k : \Omega \to \mathbb{R}^m$, $k \in \mathbb{N}$, defined on a probability space $(\Omega, \mathcal{F}, \mathbb{P})$. Thus, $\mathbf{v_k}^{-1}(F) := \{\omega \in \Omega : \mathbf{v}_k(\omega) \in F\} \in \mathcal{F}$ for all $F \in \mathbf{B}(\mathbb{R})^m$, and $\mu : \mathbf{B}(\mathbb{R}^m) \to [0,1]$ is defined as $\mu(F) := \mathbb{P}\{\omega \in \Omega : \mathbf{v}_k(\omega) \in F\}$. We restrict our attention to SHDS that satisfy the basic conditions of Definition 1. Random solutions to SHDS (C.1) are functions of $\omega \in \Omega$ denoted $\mathbf{x}(\omega)$, such that: (1) $\omega \mapsto \mathbf{x}(\omega)$ has measurability properties that are adapted to the minimal filtration of $\mathbf{v}$; (2) for each $\omega \in \Omega$ the sample path $\mathbf{x}(\boldsymbol{\omega})$ is a standard solution to the HDS (B.1) with the appropriate dependence on the random input $\mathbf{v}(\boldsymbol{\omega})$ through the jumps. To formally define these mappings, for $k \in \mathbb{Z}_{\geq 1}$, let $\mathcal{F}_k$ denote the collection of sets $\{\omega \in \Omega : (\mathbf{v}_1(\omega), \mathbf{v}_2(\omega), \ldots, \mathbf{v}_k(\omega)) \in F\}$, $F \in \mathbf{B}(\mathbb{R}^m)^k$, which are the sub-$\sigma$-fields of $\mathcal{F}$ that form the minimal filtration of $\mathbf{v} = \{\mathbf{v}_k\}_{k=1}^{\infty}$, which is the smallest σ-algebra on $(\Omega, \mathcal{F})$ that contains the pre-images of $\mathbf{B}(\mathbb{R}^m)$-measurable subsets on $\mathbb{R}^m$ for times up to k. A stochastic hybrid arc is a mapping $\mathbf{x}$ from Ω to the set of hybrid arcs, such that the set-valued mapping from Ω to $\mathbb{R}^{n+2}$, given by $\omega \mapsto \text{graph}(\mathbf{x}(\omega)) := \big\{(t,j,z) : \tilde{x} = \mathbf{x}(\omega),(t,j) \in \text{dom}(\tilde{x}), z = \tilde{x}(t,j)\big\}$, is $\mathcal{F}$-measurable with closed-values. Let $\text{graph}(\mathbf{x}(\omega))_{\leq k} := \text{graph}(\mathbf{x}(\omega)) \cap (\mathbb{R}_{\geq 0} \times \{0,1,\ldots,k\} \times \mathbb{R}^n)$. An $\{\mathcal{F}_k\}_{k=0}^{\infty}$ adapted stochastic hybrid arc is a stochastic hybrid arc $\mathbf{x}$ such that the mapping $\omega \mapsto \text{graph}(\mathbf{x}(\omega))_{\leq k}$ is $\mathcal{F}_k$ measurable for each $k \in \mathbb{N}$. An adapted stochastic hybrid arc $\mathbf{x}$ is a solution to (C.1) starting from x_0 denoted $\mathbf{x} \in \mathcal{S}_r(x_0)$ if (with $x_\omega := \mathbf{x}(\omega)$): (1) $x_\omega(0,0) = x_0$; (2) if $(t_1,j),(t_2,j) \in \text{dom}(x_\omega)$ with $t_1 < t_2$, then for almost all $t \in [t_1,t_2]$, $x_\omega(t,j) \in C$ and $\dot{x}_\omega(t,j) = f(x_\omega(t,j))$; (3) if $(t,j),(t,j+1) \in \text{dom}(x_\omega)$, then $x_\omega(t,j) \in D$ and $x_\omega(t,j+1) \in G(x_\omega(t,j), \mathbf{v}_{j+1}(\omega))$. A random solution $\mathbf{x}$ is said to be: (a) almost surely complete if for almost every sample path $\omega \in \Omega$ the hybrid arc $\mathbf{x}(\omega)$ has an unbounded time domain; and almost surely eventually discrete if for almost every sample path $\omega \in \Omega$ the hybrid arc $\mathbf{x}(\omega)$ is eventually discrete. A continuous function $V : \mathbb{R}^n \to \mathbb{R}_{\geq 0}$ is a Lyapunov function relative to a compact set $\mathcal{A} \subset \mathbb{R}^n$ for the SHDS (C.1) if $V(x) = 0 \iff x \in \mathcal{A}$, V is radially unbounded and satisfies $V(\phi(t)) \leq V(x), \quad \forall\, x \in C,\ t \in \text{dom}(\phi),\ \phi \in S_C^F(x)$, and $\int_{R^m} \max_{g \in G(x,v)} V(g)\mu(dv) \leq V(x), \quad \forall\, x \in D$, where $S_C^F(x)$ denotes the set of solutions of (C.1a) with initial condition x. The following stochastic hybrid invariance principle (Subbaraman & Teel, 2016, Thm. 8) is instrumental for our analysis.

Theorem C.1. *Let V be a Lyapunov function relative to a compact set $\mathcal{A} \subset \mathbb{R}^n$ for the SHDS system $\mathcal{H}$. Then, $\mathcal{A}$ is UGASp if and only if there does not exist an almost surely complete solution x that remains in a non-zero level set of the Lyapunov function almost surely.*

References

Bullo, F. (2019). *Lectures on network systems* (1.3 ed.). Kindle Direct Publishing, With contributions by J. Cortes, F. Dorfler, and S. Martinez.

Canavier, C. C., & Tikidji-Hamburyan, R. A. (2017). Globally attracting synchrony in a network of oscillators with all-to-all inhibitory pulse coupling. *Physical Review E*, *95*(3), Article 032215.

Chen, X., Belabbas, M. A., & Başar, T. (2017). Controllability of formations over directed time-varying graphs. *IEEE Transactions on Control of Network Systems*, *4*(3), 407–416.

Dörfler, F., & Bullo, F. (2014). Synchronization in complex networks of phase oscillators: A survey. *Automatica*, *50*(6), 1539–1564.

Gao, H., & Wang, Y. (2019). On the global synchronization of pulse-coupled oscillators interacting on chain and directed tree graphs. *Automatica*, *104*, 196–206.

Goebel, R., Sanfelice, R. G., & Teel, A. R. (2012). *Hybrid dynamical systems*. NJ: Princeton University Press.

Graham, R. L., Grötschel, M., & Lovász, L. (Eds.), (1995). *Handbook of combinatorics (Vol. 1)*. Cambridge, MA, USA: MIT Press.

Hartman, M., Subbaraman, A., & Teel, A. R. (2013). Robust global almost sure synchronization on a circle via stochastic hybrid control. In Danielle C. Tarraf (Ed.), *Lecture notes in control and information sciences*: *Vol. 449*, *Control of cyber-physical systems* (pp. 3–21). Springer.

Javed, M. U., Poveda, J. I., & Chen, X. (2019). Global synchronization of clocks in directed rooted acyclic graphs: A hybrid systems approach. In *2019 IEEE 58th conference on decision and control* (pp. 7352–7357).

Kannapan, D., & Bullo, F. (2016). Synchronization in pulse-coupled oscillators with delayed excitatory/inhibitory coupling. *SIAM Journal on Control and Optimization*, *54*, 1872–1894.

Kellet, C. M., & Teel, A. R. (2004). Smooth Lyapunov functions and robustness of stability for difference inclusions. *Systems & Control Letters*, *52*, 395–405.

Klinglmayr, J., Bettstetter, C., Timme, M., & Kirst, C. (2017). Convergence of self-organizing pulse-coupled oscillator synchronization in dynamic networks. *IEEE Transactions on Automatic Control*, *62*(4), 1606–1619.

Klinglmayr, J., Kirst, C., Bettstetter, C., & Timme, M. (2012). Guaranteeing global synchronization in networks with stochastic interactions. *New Journal of Physics*, *14*(7), Article 073031.

Kuramoto, Y. (1991). Collective synchronization of pulse-coupled oscillators and excitable units. *Physica D*, *50*, 15–30.

Mauroy, A., & Sepulchre, R. (2012). Contraction of monotone phase-coupled oscillators. *Systems & Control Letters*, *61*(11), 1097–1102.

Mayhew, C. G. (2010). *Hybrid control for topologically constrained systems* (Ph.D. dissertation), Santa Barbara: University of California.

Nishimura, J. (2013). *Designing pulse coupled oscillators to synchronize* (Ph.D. dissertation), Cornell University.

Nishimura, J., & Friedman, E. J. (2011). Robust convergence in pulse-coupled oscillators with delays. *Physical Review Letters*, *106*(19), 1606–1619.

Nishimura, J., & Friedman, E. J. (2012). Probabilistic convergence guarantees for type-II pulse-coupled oscillators. *Physical Review E*, *86*(2), 1606–1619.

Nunez, F., Wang, Y., & Doyle, F. J. (2015a). Global synchronization of pulse-coupled oscillators interacting on cycle graphs. *Automatica*, *52*, 202–209.

Nunez, F., Wang, Y., & Doyle, F. J. (2015b). Synchronization of pulse-coupled oscillators on (strongly) connected graphs. *IEEE Transactions on Automatic Control*, *60*(6), 1710–1715.

Nunez, F., Wang, Y., Teel, A. R., & Doyle, F. J. (2016). Synchronization of pulse-coupled oscillators to a global pacemaker. *Systems & Control Letters*, *88*, 75–80.

Ochoa, D. E., Poveda, J. I., Uribe, C. A., & Quijano, N. (2021). Robust optimization over networks using distributed restarting of accelerated dynamics. *IEEE Control Systems Letters*, *5*(1), 301–306. http://dx.doi.org/10.1109/LCSYS.2020.3001632.

Pagliari, R., & Scaglione, A. (2011). Scalable network synchronization with pulse-coupled oscillators. *IEEE Transactions on Mobile Computing*, *10*(3), 392–405.

Phillips, S., Sanfelice, R., & Erwin, R. S. (2012). On the synchronization of two impulsive oscillators under communication constraints. In *Proc. of American control conference* (pp. 2443–2448).

Poveda, J. I., & Teel, A. R. (2019a). Hybrid mechanisms for robust synchronization and coordination of multi-agent networked sampled-data systems. *Automatica*, *99*, 41–53.

Poveda, J. I., & Teel, A. R. (2019b). Hybrid online learning control in networked multiagent systems: A survey. *International Journal of Adaptive Control and Signal Processing3*, *33*, 228–261.

Proskurnikov, A. V., & Cao, M. (2017). Synchronization of pulse-coupled oscillators and clocks under minimal connectivity assumptions. *IEEE Transactions on Automatic Control*, *62*, 5873–5879.

Rockafellar, R. T., & Roger, J. W. (1998). *Variational analysis*. Springer-Verlag.

Sanfelice, R. G., Goebel, R., & Teel, A. R. (2007). Invariance principles for hybrid systems with connections to detectability and asymptotic stability. *IEEE Transactions on Automatic Control*, *52*, 2282–2297.

Sarlette, A., & Sepulchre, R. (2009). Consensus optimization on manifolds. *SIAM Journal on Control and Optimization*, *48*(1), 56–76.
Sepulchre, R., Paley, D. A., & Leonard, N. E. (2007). Stabilization of planar collective motion: All-to-all communication. *IEEE Transactions on Automatic Control*, *52*(5), 811–824.
Sontag, E. (1999a). Clocks and insensitivity to small measurement errors. *ESAIM. Control, Optimisation and Calculus of Variations*, *4*(4), 537–557.
Sontag, E. (1999b). Stability and stabilization: Discontinuities and the effect of disturbances. In *NATO science series*: *Vol. 528*, *Nonlinear analysis, differential equations and control* (pp. 551–598).
Subbaraman, A., & Teel, A. R. (2016). Recurrence principles and their application to stability theory for a class of stochastic hybrid systems. *IEEE Transactions on Automatic Control*, *61*(11), 3477–3492.
Teel, A. R. (2013). Lyapunov conditions certifying stability and recurrence for a class of stochastic hybrid systems. *Annual Reviews in Control*, *37*(1), 1–24.
Teel, A. R., & Poveda, J. I. (2015). A hybrid systems approach to global synchronization and coordination of multi-agent sampled-data systems. In *Proc. of analysis and design of hybrid systems* (pp. 123–128).
Teel, A. R., Subbaraman, A., & Sferlazza, A. (2014). Stability analysis for stochastic hybrid systems: A survey. *Automatica*, *50*, 2435–2456.
Tyrrell, A. (2009). Decentralized slot synchronization for cellular mobile radio. *NTT DoCoMo Technical Journal*, *10*(1), 60–67.
Wang, Y., & Doyle, F. J. (2012). Optimal phase response functions for fast pulse-coupled synchronization in wireless sensor networks. *IEEE Transactions on Signal Processing*, *60*(10), 5583–5588.
Wang, Y., Nunez, F., & Doyle, F. J. (2012). Energy-efficient pulse-coupled synchronization strategy design for wireless sensor networks through reduced idle listening. *IEEE Transactions on Signal Processing*, *60*(10), 5293–5306.
Wang, Y., Nunez, F., & Doyle, F. J. (2013). Increasing sync rate of pulse-coupled oscillators via phase response function design: Theory and application to wireless networks. *IEEE Transactions on Control Systems Technology*, *21*(4), 1455–1462.
Wang, Z., & Wang, Y. (2018). Pulse-coupled oscillators resilient to stealthy attacks. *IEEE Transactions on Signal Processing*, *66*(12), 3086–3099.
Wang, Z., & Wang, Y. (2020a). An attack-resilient pulse-based synchronization strategy for general connected topologies. *IEEE Transactions on Automatic Control*, *65*(9), 3784–3799. http://dx.doi.org/10.1109/TAC.2020.2977913.
Wang, Z., & Wang, Y. (2020b). Global synchronization of pulse-coupled oscillator networks under byzantine attacks. *IEEE Transactions on Signal Processing*, *68*, 3158–3168. http://dx.doi.org/10.1109/TSP.2020.2993643.
Wang, H., Yu, W., Ren, W., & Lu, J. (2019). Distributed adaptive finite-time consensus for second-order multiagent systems with mismatched disturbances under directed networks. *IEEE Transactions on Cybernetics*, 1–12. http://dx.doi.org/10.1109/TCYB.2019.2903218.

Muhammad Umar Javed received in 2017 his B.S. degree in Electrical Engineering with minors in Computer Science (AI/ML) and Psychology from the Lahore University of Management Sciences, Pakistan. Currently, he is a Ph.D. candidate in the Department of Electrical, Computer and Energy Engineering at the University of Colorado, Boulder, where he completed his MS in Electrical Engineering in 2019.

Jorge I. Poveda is an Assistant Professor in the ECEE Department at CU Boulder. He received the M.Sc. and Ph.D. degrees in Electrical and Computer Engineering in 2016 and 2018 from UC Santa Barbara, where he was also awarded the CCDC Outstanding Scholar Fellowship and the Best Ph.D. Dissertation Award. Before joining CU Boulder in 2019, he was a Postdoctoral Fellow at Harvard University. In 2020 he received the NSF Research Initiative Initiation Award (CRII).

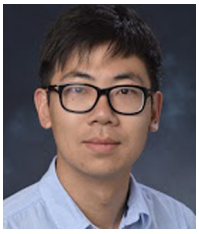

Xudong Chen is an Assistant Professor in the ECEE Department at CU Boulder. Before that, he was a postdoctoral fellow in the Coordinated Science Laboratory at the University of Illinois, Urbana–Champaign. He obtained the Ph.D. degree in Electrical Engineering from Harvard University in 2014. Dr. Chen is an awardee of the 2020 Air Force's Young Investigator Research Program, a recipient of the 2021 NSF Career Award, and the recipient of the 2021 Donald P. Eckman Award.